Review Article **Open Access**

Koji Sugioka*

Progress in ultrafast laser processing and future prospects

DOI 10.1515/nanoph-2016-0004
Received August 31, 2015; accepted December 2, 2015

Abstract: The unique characteristics of ultrafast lasers have rapidly revolutionized materials processing after their first demonstration in 1987. The ultrashort pulse width of the laser suppresses heat diffusion to the surroundings of the processed region, which minimizes the formation of a heat-affected zone and thereby enables ultrahigh precision micro- and nanofabrication of various materials. In addition, the extremely high peak intensity can induce nonlinear multiphoton absorption, which extends the diversity of materials that can be processed to transparent materials such as glass. Nonlinear multiphoton absorption enables three-dimensional (3D) micro- and nanofabrication by irradiation with tightly focused femtosecond laser pulses inside transparent materials. Thus, ultrafast lasers are currently widely used for both fundamental research and practical applications. This review presents progress in ultrafast laser processing, including micromachining, surface micro- and nanostructuring, nanoablation, and 3D and volume processing. Advanced technologies that promise to enhance the performance of ultrafast laser processing, such as hybrid additive and subtractive processing, and shaped beam processing are discussed. Commercial and industrial applications of ultrafast laser processing are also introduced. Finally, future prospects of the technology are given with a summary.

1 Introduction and history

Ultrafast lasers, which is a generic term for picosecond and femtosecond lasers, have created a new path to laser processing of materials in terms of the capabilities in ultrahigh precision micro- and nanofabrication of not only opaque but also transparent materials and three-dimensional (3D) and volume processing [1, 2]. The pulse width of ultrafast lasers is defined as several tens of femtoseconds to tens of picoseconds, where a pulse width shorter than picoseconds is typically used for fundamental research, while longer pulses are used for commercial and industrial applications because of the high output power and high reliability. Such ultrashort pulse widths suppress heat diffusion to the surroundings of processed regions, which significantly reduces the formation of a heat-affected zone (HAZ) and enables ultrahigh precision micro- and nanofabrication of a variety of materials [3, 4]. Owing to the ultrashort pulse width, the peak intensity of ultrafast lasers easily exceeds several tens of PW/cm^2, which can induce nonlinear multiphoton absorption in transparent materials. This specific feature of ultrafast lasers enables the processing of transparent materials with ultrahigh precision [5, 6]. In addition, if the focus position of the ultrafast laser beam is set inside a transparent material, then multiphoton absorption can be confined to a region near the focal volume to implement internal modification and 3D micro- and nanofabrication of transparent materials [7–9]. Thus, since the first demonstration of femtosecond laser ablation in 1987 [10, 11], research and development with regard to ultrafast laser processing has rapidly advanced.

Figure 1 shows the evolution of the number of papers related to ultrafast laser processing presented at the SPIE LAMOM conference each year. LAMON is an abbreviation for Lasers Applications in Microelectronic and Optoelectronic Manufacturing, which is a part of SPIE Photonics West and is one of the most important conferences with a long history of 20 years dealing with laser micro- and nanoprocessing. Although the number of papers related to ultrafast laser processing was few in the 1990s, it has significantly increased with a ratio of 20–30% when entering the 2000s. In the 2010s, almost half of the papers presented at SPIE LAMOM involved the use of ultrafast lasers. This analysis clearly confirms the rapid spread of ultrafast lasers in materials processing. The situation is the same for other major conferences including the Conference on Laser Ablation (COLA) and the International Symposium on Laser Precision Microfabrication (LPM).

***Corresponding Author: Koji Sugioka:** RIKEN Center for Advanced Photonics, Wako, Saitama 351-0198, Japan,
E-mail: ksugioka@riken.jp

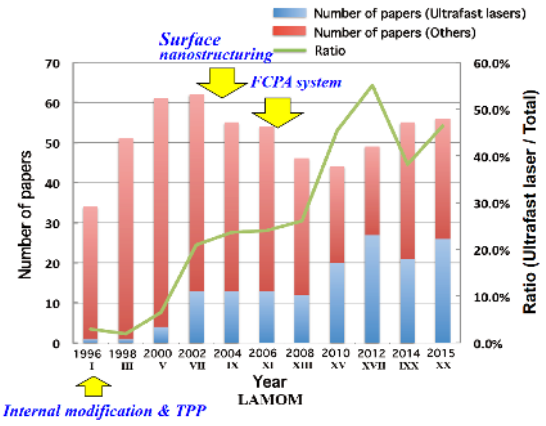

Figure 1: Evolution of the number of papers related to ultrafast laser processing presented at the SPIE LAMOM conference each year since 1996.

Looking back at the history of ultrafast laser processing, it was initiated in 1987 by the Srinivasan [10] and Stuke groups [11]. Both of these groups demonstrated clean polymer ablation using femtosecond excimer lasers almost without the formation of an HAZ and with a significant reduction of the ablation threshold compared with nanosecond lasers. Two years later in 1989, Stuke's group further demonstrated clean ablation of transparent materials because of multiphoton absorption [5]. These results surprised many researchers; however, femtosecond UV excimer lasers were used in the early stage of research on ultrafast laser processing and were not easily accessible to many researchers. In the early 1990s, the ultrafast laser became more readily accessible to more researchers because of the development of chirped-pulse amplification (CPA) in Ti:sapphire regenerative amplifiers [12, 13], which contributed to a push in fundamental research on ultrafast laser processing. In 1996, a major breakthrough in ultrafast laser processing was made by Hirao's group with the internal modification of glass with a refractive index increase by 10^{-2} to 10^{-3} based on multiphoton absorption [7]. In the same year, Mazur's group also found that focusing an ultrafast laser beam inside glass with higher pulse energy created nanovoids at the focal volumes [8]. In 1997, multiphoton absorption with ultrafast lasers was introduced into laser stereolithography, which is classified as additive 3D manufacturing, that is, 3D printing, by Kawata's group [14]. The use of a near-infrared (IR) femtosecond laser for stereolithography enables the direct creation of 3D micro- and nanostructures based on two-photon polymerization (TPP) of photocurable resins. Such internal processing of transparent materials and direct 3D micro- and nanofabrication are only available with ultrafast lasers, so that the research on ultrafast laser processing was further expanded in the 2000s. In the early 2000s, a new phenomenon associated with the interaction between ultrafast lasers and materials was found, which was the formation of nanoripples with periodicities of 1/10 to 1/2 of the incident laser wavelength formed by the multiple pulse irradiation of linearly polarized ultrafast laser beams [15–17]. In the late 2000s, nanoablation using metal and dielectric nanospheres was demonstrated for the fabrication of subwavelength structures by near-field enhancement near the nanospheres [18, 19]. Both techniques are being extensively investigated with the expectation of diverse applications. In addition, the improvement in the performance of ultrafast laser systems in the 2000s has been a significant contribution to realizing more reliable ultrafast laser processing for practical use. A robust, stable, and very compact fiber chirped pulse amplifier (FCPA) was developed in 2006 [20] and has expanded the range of applications. Furthermore, a compact and high-power ultrafast laser system based on a rare-earth-doped laser medium by diode pumping was developed in 2008 and is applicable to industrial applications, although the typical pulse width was in the order of picoseconds [21, 22].

From the efforts to date, ultrafast laser processing is becoming a reliable and powerful tool for commercial and industrial applications in the 2010s, while fundamental research is also increasingly active. Thus, ultrafast lasers are currently used widely for both fundamental research and practical applications. Here, a comprehensive review is presented on the progress in ultrafast laser processing, including micromachining, surface micro- and nanostructuring, nanoablation, and 3D and volume processing. Advanced technologies to enhance the performance of ultrafast laser processing are discussed, and commercial and industrial applications of ultrafast laser processing are also introduced. Finally, future prospects of the technology are given with a summary.

2 Micromachining

One of the important characteristics of ultrafast lasers in terms of materials processing is the nonthermal process associated with the elimination of heat diffusion to minimize the formation of an HAZ at the surroundings of processed regions owing to the ultrashort pulse width, which enables clean, ultrahigh precision machining of a diversity of materials from metals with high thermal conductivity to polymers with low thermal resistance. The multiphoton absorption induced by the extremely high peak intensity

can also be adopted to achieve high-quality machining of brittle transparent materials such as glass.

Figure 2 shows scanning electron microscopy (SEM) images of various samples machined with a femtosecond laser including (a) microdrilling of stainless steel, (b) groove formation in polymethyl methacrylate (PMMA), and (c) flexible cleaving of fused silica [23]. Regardless of the material, the femtosecond laser performed clean ablation with sharp edges and without the formation of an HAZ or cracks. Such excellent micromachining features lead to ultrafast laser processing being applied to the drilling of through-holes, scribing and cutting, surface pattering and microstructuring, and trimming, with extensive commercial and industrial applications as introduced in Section 9.

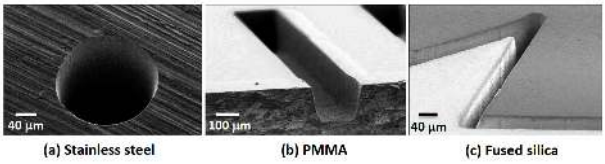

Figure 2: SEM images of different kinds of samples machined with a femtosecond laser, including (a) microdrilling of stainless steel, (b) groove formation in polymethyl methacrylate (PMMA), and (c) flexible cleaving of fused silica (courtesy of M. Gower).

3 Surface micro- and nanostructuring

Different types of micro- and nanostructures can be formed on the surfaces of various types of materials by interaction with ultrafast laser beams according to conditions such as the laser intensity, polarization, spatial and temporal beam profiles, laser wavelength, and processing atmosphere. In this section, the two most practical structures are introduced.

It is well known that parallel ripple structures are formed on the surfaces of various types of materials with multiple pulse irradiation of a linearly polarized laser beam with nanosecond or longer pulses [24, 25]. Such structures are called laser-induced periodic surface structure (LIPPS). LIPPS is considered to be formed by interference of the incident laser beam with the light scattered or reflected at the surface. Consequently, the direction of the parallel ripples formed is always perpendicular to the polarization of the incident laser beam. In addition, the spatial period of the LIPPS is close to the incident laser wavelength. In contrast, multiple pulse irradiation (several tens to several hundreds of pulses) from an ultrafast laser with a laser fluence near the ablation threshold produces high-spatial-frequency LIPPS (HSFL) on a variety of materials including metals, ceramics, semiconductors, insulators, and polymers [15–17, 26, 27]. The spatial period of the formed ripple is much smaller than the laser wavelength (typically 1/10–2/5 of λ) and is dependent on the type of material and the irradiation conditions. At higher laser fluence, the period increases to more than 2/5 of λ, but is still smaller than the wavelength, which is referred to as low-spatial-frequency LIPPS (LSFL). Mechanisms for nanoripple formation has been extensively investigated, and include the self-organization of surface instability [28], second-harmonic generation [17], refractive index change [29], nanoplasma formation [30], and the excitation of surface plasmon polaritons [31]; however, the mechanism is still under debate. The formed nanoripples are expected to be applied to reduce the friction between moving components, reduce the adhesive force of micro- and nanocomponents, and increase the adhesion of thin films and medical implants, increase wettability, the orientation of living cells, and surface coloring and painting. Figure 3 shows an example of color printing on a stainless steel surface by nanoripple formation using a femtosecond laser [32]. The color effect is achieved by the diffraction of light from the periodic nanostructures formed on the surface [33, 34]. Spatial control of the nanostructure orientation, which is dependent on the polarization direction, enables the successful imprinting of color images on the metal surface.

Another interesting and practical structure is formed by several-hundred-pulse irradiation from a femtosecond laser in a halogen gas such as SF_6 and Cl_2 [35, 36], and results in a quasi-ordered array of micrometer-sized, conical structures (Fig. 4(c, d)). The size and shape of the formed microstructures is dependent on the laser fluence, wavelength and pulse duration, as well as the type and pressure of the background gas. The structures produced can strongly reduce reflection of incident light, so that the metallic mirror finish of an Si surface is changed to a deep matte black color (Fig. 4(a)), which is termed black silicon. This structure increases absorption, even in the infrared region [37, 38]. Thus, such a textured Si surface is beneficial to enhance the efficiency of photovoltaic solar cell applications [39]. Similar structures can be produced on not only Si but also other semiconductors and metals [40–42]. A possible mechanism for the formation of this type of structure has been proposed, involving anomalous density behavior of the solid and molten materials when the phase is changed by laser irradiation [43]. In addition to the elim-

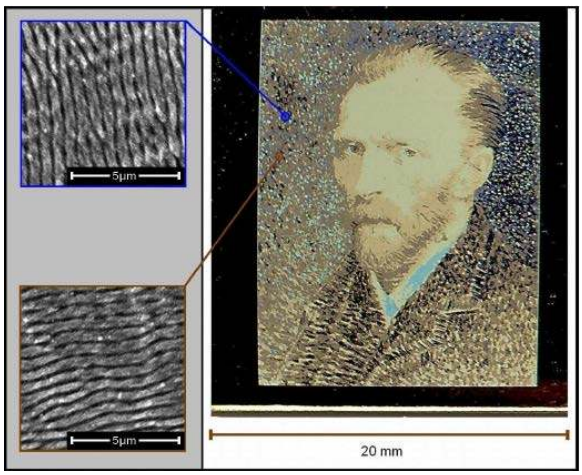

Figure 3: (a) Color printing on a stainless steel surface by nanoripple formation using a femtosecond laser. The image was obtained using a typical reading scanner. (b) SEM images of controlled nanostructures with different orientations created at different positions and showing different colors [32]. Reproduced with permission from The Optical Society of America, ©2010 by The Optical Society of America.

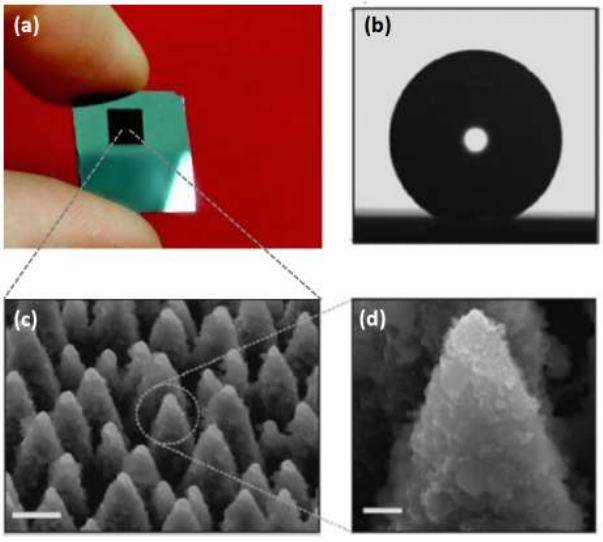

Figure 4: (a) Photograph of a black Si area where a Si substrate was textured using a femtosecond laser in a halogen atmosphere. Courtesy of Emmanuel I. Stratakis. (b) Static contact angle measurement of a 0.78-mm radius water droplet on the textured surface; the contact angle was measured as about 154°. (c) SEM image of the textured surface comprised of protrusions with conical or pyramidal asperities with average sizes of about 10 μm at a surface density of 1.0×10^6 cm^{-2} (scale bar 5 μm). (d) Magnified image of a single protrusion in (c), which depicts nanostructures with sizes up to few hundred nanometers on the slopes of the protrusions (scale bar 1 μm) [44]. Reproduced with permission from Wiley, ©2008 by Wiley.

ination of light reflection, this type of structure quantitatively mimics both the structure and water-repellent characteristics of the natural Lotus leaf, thereby exhibiting superhydrophobicity because of the lotus effect, as shown in Fig. 4(b) [44]. Some of the applications of this characteristics include self-cleaning products, in addition to microfluidics and tissue engineering.

4 Nanoablation

The excellent characteristics of ultrafast laser processing with respect to the suppression of thermal diffusion, which thereby reduces the HAZ, enables nanoablation to be performed with subwavelength resolution or smaller. Such a high fabrication resolution beyond the diffraction limit of laser beams is achieved because of the threshold effect when using a Gaussian beam. Higher fabrication resolution can be obtained by a decrease in the laser intensity where only the central part of laser beam with a Gaussian profile can exceed the threshold to induce ablation. The use of multiphoton absorption can further improve the fabrication resolution, where the effective diameter ω for n-photon absorption is given by

$$\omega = \omega_o/\sqrt{n}, \tag{1}$$

because the effective absorption coefficient for n-photon absorption is proportional to nth power of the laser intensity. Here, ω_o is the actual beam diameter of the focused Gaussian laser beam [1, 2, 45]. A two-dimensional (2D) array of nanoholes with diameters smaller than 200 nm was formed on a GaN surface by femtosecond laser ablation at a wavelength of 387 nm based on two-photon absorption using an objective lens with a numerical aperture (NA) of 0.9 [46, 47].

In principle, using the threshold effect offers no limitation to the improvement that can be achieved in the fabrication resolution by precise control of the laser intensity. However, the pulse-to-pulse fluctuation in femtosecond laser pulse energy makes it extremely difficult to maintain the same fabrication resolution when the laser intensity is near the threshold intensity. Therefore, the reproducible fabrication resolution is limited to 100–200 nm. To achieve super high resolution far beyond the diffraction limit, novel irradiation methods have been developed, which are described in the following.

4.1 Near-field ablation

One solution to overcome the diffraction limit is to use the optical near field. The laser irradiation combined with advanced tools such as (a) apertureless-pointed tips used for scanning tunneling microscopy (STM) and atomic force microscopy (AFM), (b) apertured tips used for near-field scanning optical microscopy (NSOM), and (c) dielectric and metal nanospheres, as shown in Fig. 5, induce a strong optical near field to achieve nanoablation with feature sizes much smaller than 100 nm [48]. The nanomachining of gold thin films with a high spatial resolution of ca. 10 nm was demonstrated by local field enhancement in the near-field around the AFM tip with irradiation from a 800-nm wavelength femtosecond laser [49]. The combination of a 260-nm wavelength femtosecond laser with an NSOM tip was used to remove a 100-nm thick chrome layer from a quartz substrate for application to photolithographic mask repair with nanometric resolution [50].

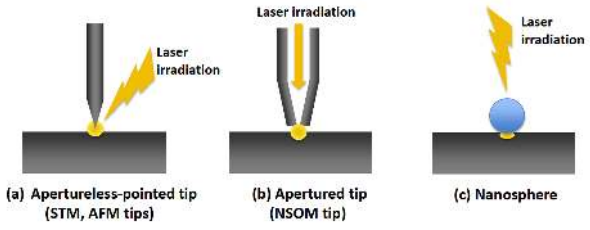

Figure 5: Schematic diagrams of three schemes for nanoablation using the optical near-field. (a) Apertureless-pointed tips used for scanning tunneling microscopy (STM) and atomic force microscopy (AFM), (b) apertured tips used for near-field scanning optical microscopy (NSOM), and (c) dielectric and metal nanospheres.

Recently, nanoablation using nanospheres has been more extensively investigated [18, 19]. The mechanism of nanoablation beyond the diffraction limit is attributed to the near-field enhancement near the nanospheres. Both metal and dielectric nanospheres are available for nanoablation to generate an intense near field mainly by Mie scattering. The underlying process to generate an intense near field by the metal nanospheres is ascribed to free electron oscillation (plasmons), while it is ascribed to scattered light for dielectric nanospheres. Figure 6 shows SEM images of nanoholes created on SiO_2 (Figure 6a) and Si (Figure 6b) substrates by irradiation from a 400-nm wavelength femtosecond laser with amorphous TiO_2 nanospheres of 200 nm in diameter [51]. A circular nanohole with a diameter of 90 nm was created on SiO_2 with a laser fluence of 1.4 mJ/cm^2, which is significantly lower than the half ablation threshold of the bare substrate (3.8 J/cm^2). A circular nanohole with a diameter of 100 nm could also be created on the Si substrate with almost half the laser fluence (40 mJ/cm^2) of the substrate ablation threshold.

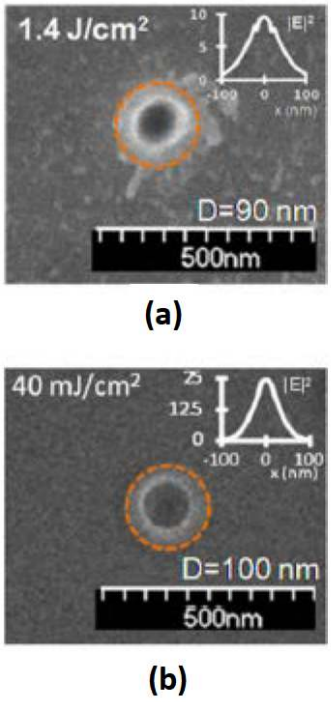

Figure 6: SEM images of nanoholes created on SiO_2 and Si substrates by single pulse irradiation from a 400-nm wavelength femtosecond laser using 200-nm diameter nanospheres of amorphous TiO_2. The dashed line shows the delineation of the applied nanospheres [51]. Reproduced with permission from The American Institute of Physics,

4.2 Far-field ablation

The use of the optical near-field can overcome the diffraction limit to realize nanoprocessing. However, the laser intensity exponentially decays in the vicinity of nanoprobes and nanospheres. Thus, the ablation depth is shallower than 100 nm, which results in nanoholes with an aspect ratio much smaller than 1 [52]. In contrast, far-field ablation is, in principle, free from this restriction.

As described in Section 3, periodic nanoripple structures can be formed on material surfaces by irradiation with a linearly polarized ultrafast laser beam. This is ascribed to spatial modulation of the energy deposition on the surface with nanoscale periodicity at the focal spot, as shown in Fig. 7(a). When the laser intensity is reduced, the

number of cycles of the modulated energy distribution decreases (Fig. 7(b)). Further reduction to a level very near to the ablation threshold results in only a single cycle of the modulated energy distribution in the central area of the focal volume (Fig. 7(c)), which creates a single line nanogroove [53–56].

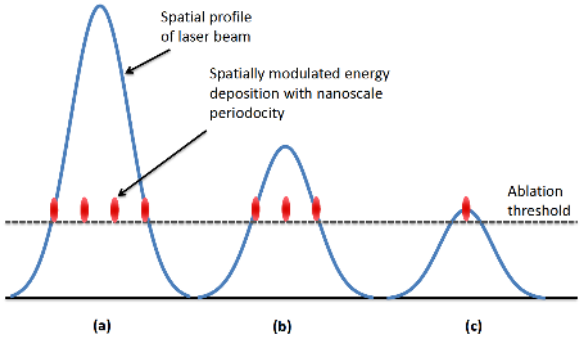

Figure 7: Schematics for spatially modulated energy deposition with nanoscale periodicity at the focal spot. As the pulse energy is reduced, the number of cycles of the modulated energy distribution decreases.

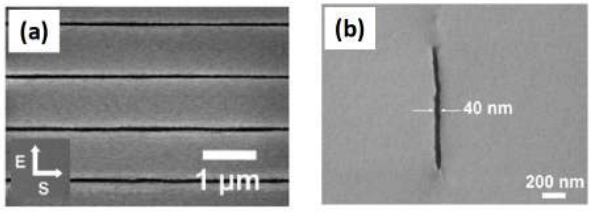

Figure 8: SEM images of (a) an array of single nanogrooves with widths less than 40 nm fabricated on ZnO [56]. Reproduced with permission from The Optical Society of America, ©2014 by The Optical Society of America. (b) Cross-sectional SEM image of a nanochannel with a width of about 40 nm and a depth of about 40 μm (aspect ratio: ca. 1000) formed inside porous glass by ablation in water [54].

Using this scheme, an array of single nanogrooves with widths less than 40 nm were fabricated on ZnO, as shown in the SEM image of Fig. 8(a) [56]. To write a single groove line, the focused laser beam was scanned along the direction perpendicular to the laser beam polarization. After single line writing, the focused laser beam was shifted parallel to the polarization direction with a spacing of 1 μm to write the next line. Periodic nanoripple structures can also be formed inside glass [57]. Figure 8(b) shows an SEM image of a nanochannel with a width of ca. 40 nm and a depth of ca. 40 μm (aspect ratio of ca. 1000) formed inside porous glass by ablation in water using a linearly polarized femtosecond laser beam with precise control of the laser intensity [54]. These fabricated nanochannels were applied to DNA analysis, such as in the stretching of DNA molecules.

5 Two-photon polymerization

Focusing a near-IR femtosecond laser in a photocurable epoxy resin enables the formation of 3D micro- and nanostructures because of the internal modification based on two-photon absorption [14, 45]. Stereolithography performed using a near-IR femtosecond laser is termed TPP and is unlike conventional stereolithography that uses UV light for the layer-by-layer creation of 3D structures with shifting the elevator stage. Instead of a photocurable resin, a solid resist can also be adopted for TPP. Unlike photocurable resin, the solid resist enables both bottom-up fabrication (additive manufacturing) [58] and top-down fabrication (subtractive manufacturing) [59] by the selection of negative- or positive-tone photoresists, respectively.

5.1 Challenges to fabrication resolution far beyond the diffraction limit

One prominent feature of TPP is the high fabrication resolution beyond the optical diffraction limit, which is achievable by a combination of the threshold effect and the reduction of the effective beam diameter because of two-photon absorption, as described in Section 4. The typical fabrication resolution of TPP using a high NA objective lens (ca. 1.4) in a plane perpendicular to the laser beam axis (lateral resolution) is 100–200 nm, despite the IR laser wavelength of ca. 800 nm [45]. Precise control and stabilization of the laser intensity very close to the TPP threshold, together with an optimal writing speed, has enabled a fabrication resolution down to ca. 18 nm [60]. A more sophisticated approach to further improve the fabrication resolution in TPP was conducted by adopting the concept of stimulated emission depletion (STED) microscopy, which was originally developed for far-field nanoimaging of live cells [61]. This approach involves simultaneous irradiation with an activation beam, such as that with a wavelength of 800 nm and a pulse width of 200 fs, which induces photopolymerization in a negative-tone photoresist, and a deactivation beam operated at the same wavelength but in continuous wave mode, which is superimposed on the activation beam with a suitable lateral off-

set to deactivate the photoinitiator [62]. This technique has been termed STED lithography or resolution augmentation through photo-induced deactivation (RAPID) lithography. In typical RAPID lithography, a doughnut-shaped deactivation beam is used to inhibit photopolymerization triggered by the activation beam at the doughnut ring that corresponds to the outer part of the activation beam, which results in the improvement of the fabrication resolution to less than 100 nm. The development of a photocurable resin with high mechanical strength is an important factor to achieve higher fabrication resolution. By using the developed, high-mechanical-strength resin and increasing the power of the doughnut-shaped deactivation beam, the width of the written polymer line has been decreased down to 9 nm, as shown in Fig. 9 [63]. However, 3D nanostructures with such super high resolution have not yet been successfully produced using RAPID lithography.

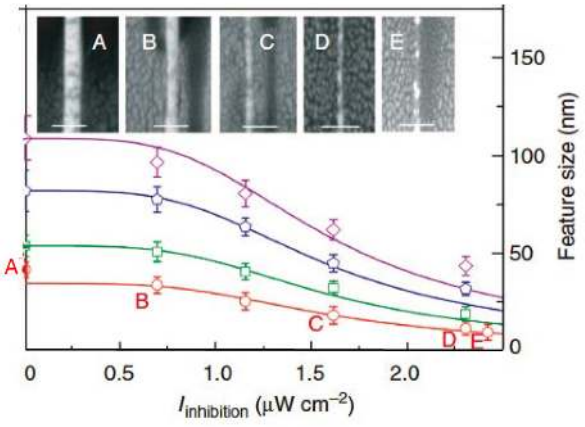

Figure 9: Dependence of the feature size of free-standing polymer lines written by RAPID lithography on the intensity of the doughnut-shaped deactivation beam. Insets show SEM images of points A, B, C, D, and E (scale bar: 100 nm) [63]. Reproduced with permission from Nature Publishing Group, ©2013 by Nature Publishing Group.

5.2 Applications

The exceptional characteristics of TPP that enable 3D rapid prototyping with nanometric fabrication resolution have been extensively applied to fabricate microoptical components [64], photonic crystals [58, 65, 66], micro- and nanosystems [67–69], microfluidic devices [70–72], medical devices [73], and scaffold for tissue engineering [64, 73, 75]. Figure 10 shows examples of 3D micro- and nanostructures fabricated using TPP: (a) a 2 × 2 array of plano-convex microlens [64], (b) a photonic bandgap crystal [66],

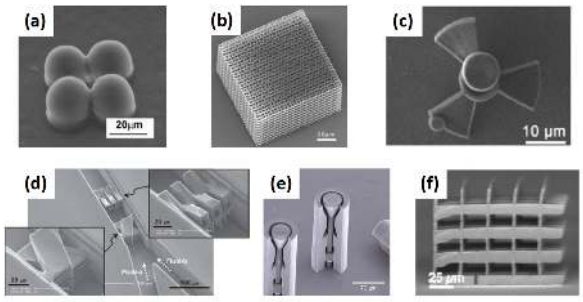

Figure 10: Three-dimensional micro- and nanostructures fabricated by TPP. (a) A 2×2 array of plano-convex microlenses [64], reproduced with permission from The Optical Society of America, ©2006 by The Optical Society of America. (b) Photonic bandgap crystal [66], reproduced with permission from Wiley. ©2005 by Wiley. (c) Microturbine that can be rotated by application of an external magnetic field [69], reproduced with permission from The Royal Society of Chemistry, ©2010 by The Royal Society of Chemistry. (d) Fluid-mixing components integrated in an open microfluidic channel [72], reproduced with permission from The Royal Society of Chemistry, ©2011 by The Royal Society of Chemistry. (e) Microvalve designed to prevent reversal of blood flow in human veins [73], reproduced with permission from Nature Publishing Group, ©2009 by Nature Publishing Group. (f) Twenty-five-μm pore-sized scaffold for 3D cell migration study [75], reproduced with permission from Wiley, ©2008 by Wiley.

(c) a microturbine that is rotated by application of an external magnetic field [69], (d) fluid-mixing components integrated into an open microfluidic channel [72], (e) a microvalve designed to prevent reflux of blood flow in human veins [73], and (f) a 25-μm pore-sized scaffold for 3D cell migration studies [75].

Resins typically used for TPP are SCR 500, SU-8, and NOA 61, which produce standard polymers with no specific functions. Optical, electrical, magnetic, or mechanical functions can be incorporated into the formed polymers by doping the common resins with special substances. For example, 3D multicolor luminescent polymer microstructures were produced by the incorporation of CdS nanoparticles (cadmium methacrylates) [76]. Doping with surface-modified Fe_3O_4 nanoparticles imparted magnetic properties to 3D polymer microstructures [77]. Single-wall carbon nanotubes (SWCNTs)/polymer composites with arbitrary 3D micro- and nanostructures were synthesized from a mixture of an SWCNT solution and the resin [78], where the SWCNTs in the composite structure were aligned with the laser scanning direction.

6 Internal and volume processing of transparent materials

One of the most distinct features of ultrafast laser processing is the capability of 3D and volume processing inside transparent materials in a spatially selective manner because of multiphoton absorption associated with the extremely high peak intensity [7–9]. When an ultrafast laser beam is focused inside a transparent material with an adequate pulse energy, multiphoton absorption can be confined to a region near the focal volume inside the material, only where the laser intensity exceeds the critical value to efficiently induce multiphoton absorption. In this way, internal modification and 3D processing of transparent materials can be performed. Such processing, unique to ultrafast lasers, includes refractive index modification [7], nanovoid formation, [8], valence state change of doped ions [79], elemental redistribution in materials [80], atom precipitation [81], particle crystallization [82], and enhancement of the chemical etching rate [83].

6.1 3D photonic devices

Ultrafast laser processing has been extensively applied to fabricate 3D photonic devices such as optical couplers and splitters [84], volume Bragg gratings [85], diffractive lenses [86], Mach–Zehnder interferometers (MZIs) [87], and waveguide lasers [88, 89]. Such photonic devices rely on the writing of 3D optical waveguides that can be easily inscribed in transparent materials such as glass, crystalline materials, and polymers by inducing permanent refractive index changes in the focal volumes of tightly focused ultrafast laser pulses [90].

Optical waveguides written using ultrafast lasers promise solutions in terms of nonplanar configuration, stability, and miniaturization of fabricated photonic devices. This distinct feature has recently attracted significant interest for application to the fabrication of compact quantum optics and circuits. A 3D multipath interferometer constructed with femtosecond laser-inscribed optical waveguides has demonstrated tunable quantum interference at the chip scale and is thus capable of quantum-enhanced phase measurements [91]. Several functional quantum photonic circuits have been built in glass chips, on which quantum information processing such as photonic boson sampling and Anderson localization (i.e., trapping of scattered fields in a disordered material) has been successfully demonstrated [92, 93]. Conventional quantum circuits for quantum information processing are constructed with bulk optics that include a large amount of discrete elements on optical tables, which suffer from a large footprint size with poor stability. In contrast, the ultrafast laser-written optical waveguides offer simple and miniaturized configurations with much more robust construction.

6.2 Data storage applications

Focusing an ultrafast laser beam with laser intensity higher than that for refractive index modification creates submicrometer-sized nanovoids in glass. Binary information based on digital bits has been successfully recorded by writing nanovoids in multiple planes with a density of 17 Gbits/cm^3 [8]. It has recently been demonstrated that the digital bits inscribed in fused silica with a femtosecond laser have a long-term data storage lifetime of more than 319 million years, which has been confirmed by the accelerated test at 1000 °C for 120 min [94]. The recording density written by holographic femtosecond laser processing using a spatial light modulator (SLM) reached 40 Mbyte/inch^2 with a dot pitch of 2.8 μm in four layers, which is greater than that of a compact disk.

As described in Sections 3 and 4, self-assembled nanogratings can be formed at the focused area by irradiation with a linearly polarized ultrafast laser beam. The formation of such complex nanostructures has realized 5D data storage because birefringence induced by the nanograting provides the fourth and fifth dimensions by the slow axial orientation and strength of retardance, respectively, in addition to the XYZ dimensions in space [95]. The slow axial orientation and the strength of retardance can be independently manipulated according to the polarization and intensity of the incident beam. In the recording procedure using fused silica with a femtosecond laser, discretized multilevel intensity control in multiple dots was conducted by SLM-generated holograms with a modified and weighted Gerchberg–Saxton (GSW) algorithm to multiplex the data by retardance, while motion-free polarization direction control was implemented using a laser-imprinted half-wave plate matrix made of four segments for control of the slow axial azimuth. The readout of the recorded data in the glass was demonstrated with a quantitative birefringence measurement system integrated with an optical microscope. Three birefringent layers with a layer interval of 20 μm were clearly distinguished in this system [Fig. 11(a)]. The phase retardance [Fig. 11(c)] and slow axis orientation [Fig. 11(d)] were then derived from Fig. 11(a). Normalized data [Fig. 11(e) and 11(f)] gave the final results [Fig. 11(g) and 11(h)]. In the ideal case, this tech-

nique that enables 5D optical storage could realize capacities up to 18 GB in a fused silica substrate, the same size as that of a conventional compact disc. The recorded data was confirmed to be thermally stable up to 1000 °C, which suggests unlimited lifetime at room temperature.

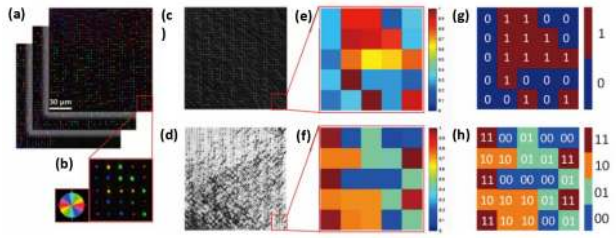

Figure 11: Five-dimensional data storage readout. (a) Birefringence measurement of the data recorded in three different layers in depth. (b) Enlarged 5 × 5 dots array. (c) Retardance distribution retrieved from the top data layer. (d) Slow axis distribution retrieved from the top data layer. (e,f) Enlarged normalized retardance matrix and slow axis matrix from (b). (g,h) Final binary data retrieved from (e) and (f) [95]. Reproduced with permission from American Physical Society, ©2008 by American Physical Society.

6.3 3D microfluidics and optofluidics

Multiphoton absorption confined to the focal volume inside glass can be used to directly create 3D microfluidic structures, thereby eliminating additional procedures usually required, including stacking and bonding of the glass substrates. Microfluidics is a key component for biochips, which are essentially miniaturized laboratories used for reactions, detection, analysis, separation, and the synthesis of biochemical materials with benefits of high sensitivity, short analysis time, low reagent consumption, and low waste production. There are two methods available for the fabrication of 3D microfluidics structures using ultrafast lasers, which are femtosecond laser-assisted etching (FLAE) [83, 96] and water-assisted femtosecond laser drilling (WAFLD) [97].

FLAE involves ultrafast laser direct writing inside glass, which space selectively modifies the chemical properties at the laser-inscribed regions, and successive chemical wet etching, typically in diluted hydrofluoric (HF) acid solution, to selectively remove the laser-modified regions (Fig. 12(a)). This two-step procedure results in the formation of 3D microfluidic structures inside glass such as photosensitive glass [96, 98, 99] and fused silica [84, 100]. The microchannels fabricated by FLAE inevitably become wider than the laser-exposed regions and are tapered because of an etch selectivity ratio of approximately 50 between the laser-exposed and laser-unexposed regions. Meanwhile, the internal wall of the fabricated hollow structure is very smooth, particularly with photosensitive glass, which allows FLAE to be extended to the fabrication of microoptics such as micromirrors and microlenses inside a glass substrate [101]. FLAE can also be used to fabricate movable micromechanical components such as microvalves and micropumps, which are free from the substrates inside the 3D microfluidic structures, because the ultrafast laser direct writing in this process simply inscribes the latent 3D images that are then developed by wet etching [102, 103].

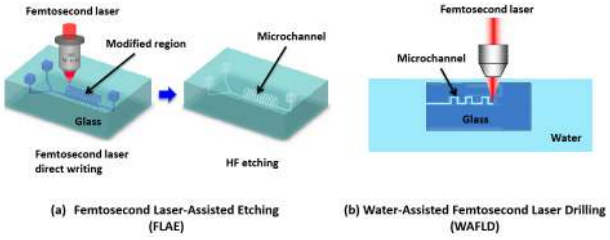

Figure 12: Schematic illustrations of two methods available for the fabrication of 3D microfluidics structures by ultrafast laser processing: (a) femtosecond laser-assisted etching (FLAE) and (b) water-assisted femtosecond laser drilling (WAFLD).

For WAFLD, a glass substrate immersed in distilled water is ablated by direct femtosecond laser writing, as shown in Fig. 12(b) [97]. The role of water in this process is to efficiently remove debris from the ablated regions, which enables the formation of long microfluidic channels with complex structures. WAFLD relies on ablation; therefore, it can provide not only better uniformity but also narrower channel diameters over a long range. Nanochannels with diameters of ca. 700 nm and arbitrary geometry have been fabricated in fused silica using low-energy femtosecond laser pulses near the ablation threshold that are tightly focused by a high-NA objective lens [104]. Further enhancement of the performance of WAFLD to fabricate microfluidic channels with almost unlimited lengths, arbitrary geometries, and widths far less than the diffraction limit has been demonstrated by the ablation of mesoporous glass immersed in water followed by post-annealing [53, 54, 105]. The pores in porous glass that form a 3D connective network enable the more efficient supply of water to the ablation site, which results in the efficient removal of debris from the ablated regions to create unprecedented micro- and nanochannels.

The versatility of ultrafast laser 3D processing makes it possible to integrate functional microcomponents such as microoptics and microelectronics into a 3D glass microfluidic system to functionalize biochips for the fabrication of optofluidics and electrofluidics [11, 106–110, 112, 113]. Figure 13(a) shows a 3D schematic illustration of an optofluidics system fabricated by femtosecond laser 3D processing, which is used to perform label-free spatially selective sensing of liquid samples [107]. In this optofluidics system, an unbalanced MZI was constructed with optical waveguides by femtosecond laser refractive index modification after fabrication of a straight microfluidic channel embedded in fused silica by FLAE. In the MZI, the reference arm passes over the microchannel, while the sensing arm intersects the microchannel at a right angle. This optofluidics device can be used to measure the refractive index with a spatial resolution in the order of the waveguide mode diameter (11 μm). The unbalanced MZI can detect fringes in the wavelength-dependent transmission when a suitable spectral region is scanned using a tunable light source. The refractive index varies slightly with the analyte concentration, and the variation can be detected by a shift in the fringe, as shown in the inset of Fig. 13(b). Consequently, this optofluidics device could be used to successfully detect a test sample of glucose-D with a concentration as low as 4 mM, which corresponds to a sensitivity of 10^{-4} refractive index units.

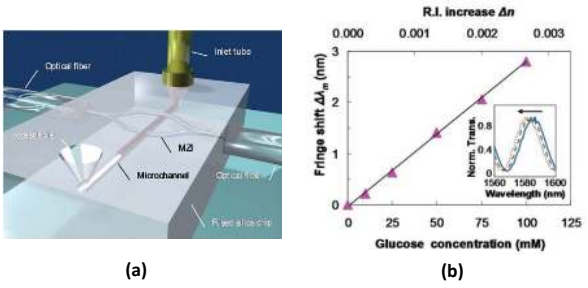

Figure 13: (a) Three-dimensional schematic illustration of optofluidics fabricated by femtosecond laser 3D processing to perform label-free spatially selective sensing of liquid samples. The sensing arm in the MZI crosses the channel orthogonally, while the reference arm passes over it. (b) Measured fringe shift for various glucose-D concentrations (inset: solid line 0 mM; dashed line 50 mM; dotted line 100 mM) measured using the fabricated optofluidic system with an unbalanced MZI. The top axis indicates the correspondent refractive index change [107]. Reproduced with permission from The Royal Society of Chemistry, ©2010 by The Royal Society of Chemistry.

6.4 Glass bonding

Glass bonding has recently attracted much interest because of its potential in applications such as electronics, optics, microelectromechanical systems (MEMS), medical devices, microfluidic devices, and small satellites. Laser fusion welding is a promising candidate for glass bonding because it can provide rapid, high-precision, high-quality, flexible features in bonding with low heat distortion. For glass bonding, the laser beam should be absorbed at the interface of stacked glass substrates. Therefore, CO_2 lasers that are conventionally used for welding cannot be used, because of strong absorption by the glass, which prevents propagation to the interface. Other conventional lasers, such as Nd:YAG lasers, fiber lasers, and laser diodes require the insertion of an intermediate absorber layer between the two glass substrates because they have low absorption in glass. In contrast, absorption from ultrafast lasers can be confined to the interface of two stacked glass substrates because of multiphoton absorption when the focal position is set at the interface. Glass bonding based on fusion welding with ultrafast lasers is considered to occur because of melting induced at the interface by heating with the multiphoton absorption of a focused laser beam. Glass bonding using a femtosecond laser was first experimentally demonstrated in 2005, in which an 800-nm, 130-fs laser at a repetition rate of 1 kHz was used to bond two fused silica substrates [114]. Since then, the femtosecond laser and also the picosecond laser have been extensively used to bond the same type of glass substrates, including fused silica [114–116], borosilicate glass [117, 118], soda-lime glass [119], nonalkali aluminosilicate glass [120], and photosensitive Foturan® glass [121], in addition to dissimilar glass substrates such as fused silica/borosilicate glass [116, 122], optical fiber/glass slide [123], and spherical glass bead/float glass [124]. The ultrafast laser welding technique has been further extended to bond glass to other materials such as Si [125] and metals [126].

7 Hybrid additive and subtractive processing

Laser processing can be classified into three categories: additive, undeformative, and subtractive manufacturing. Each process has its own advantages and disadvantages. For example, additive manufacturing using TPP with a negative-tone resist is not suitable for the formation of large volume objects because of the bottom-up fabrication. For example, to produce a 1-mm^3 volume 3D microfluidic

structure under typical TPP process conditions would require a fabrication time that exceeds 100 days. In contrast, it is quite difficult to fabricate 3D structures with complex shapes by subtractive manufacturing with ablation processes. Thus, a combination of these manufacturing processes could provide the possibility to diversify the geometry and/or enhance the functionalities of the fabrication targets. One good example has already been presented in Fig. 13, in which subtractive FLAE was combined with undeformative manufacturing for refractive index modification to realize a functional optofluidics system.

A hybrid additive and subtractive process has recently been shown to be capable of fabricating previously inaccessible 3D micro- and nanostructures [127–130]. Successive additive and subtractive fabrication processing with TPP followed by femtosecond laser multiphoton ablation was successfully demonstrated for the fabrication of submicrometer polymer fibers containing periodic holes with 500 nm diameters and 3D microfluidic channels with 1 µm diameters [127]. For the fabrication of polymer fibers containing periodic holes, TPP was first used to fabricate fiber structures with 2-, 1-, and 0.5-µm line widths, as shown in Fig. 14(a), 14(c), and 14(e), respectively. After TPP, subtractive femtosecond laser ablation formed periodic holes with ca. 500 nm diameters in the polymer fibers, which acted as Bragg grating structures in the fibers, as shown in Fig. 14(b), 14(d), and 14(f). The diameter and the periodicity of the holes were adjustable through control of the laser irradiation conditions. It should be noted that it is difficult to fabricate such fiber Bragg gratings by either TPP or femtosecond laser multiphoton ablation alone.

Another hybrid scheme involves successive subtractive FLAE and additive TPP to realize 3D ship-in-a-bottle biochips, which enables the fabrication of novel biochips by the integration of various 3D polymer micro/nanostructures into flexible 3D glass microfluidic channels [128–130]. Figure 15 shows a schematic diagram for the fabrication procedure of ship-in-a-bottle biochips by the hybrid technique, which mainly consists of FLAE of photosensitive glass (femtosecond laser direct writing followed by annealing, HF etching, a second anneal to smooth the inner surfaces) and TPP inside the microfluidic structures created by FLAE (polymer filling, femtosecond laser direct writing, and development). This novel technique has been used to fabricate microfluidic and optofluidic systems integrated with micro/nanofilters, micromixers, and microoptical components. As one example, a microlens array combined with center-pass units, which is schematically illustrated in Fig. 16(a) and shown in the SEM image of Fig. 16(b), was integrated into a closed microfluidic channel embedded in a glass substrate

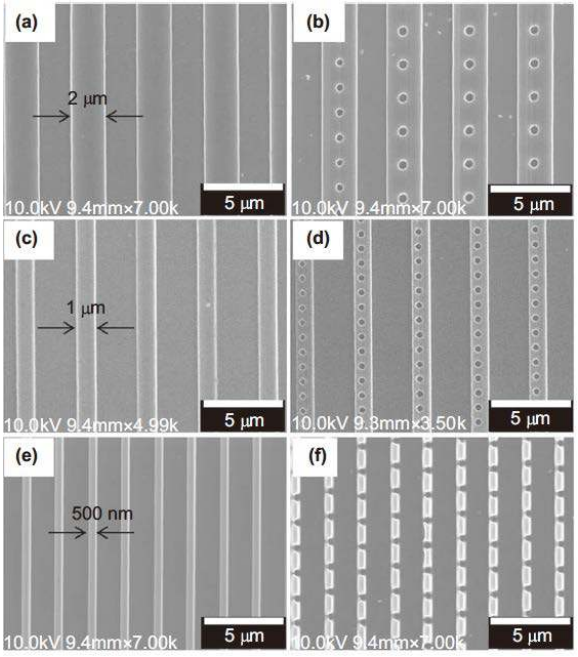

Figure 14: SEM images of polymer fibers fabricated by hybrid additive and subtractive fabrication processing using TPP followed by femtosecond laser multiphoton ablation. (a,c,e) Arrays of fibers formed using TPP with 2, 1, and 0.5 µm in diameters, respectively. (b,d,f) Arrays of fibers with periodic hole patterns formed by femtosecond laser multiphoton ablation [127]. Reproduced with permission from Nature Publishing Group, © 2012 by Nature Publishing Group.

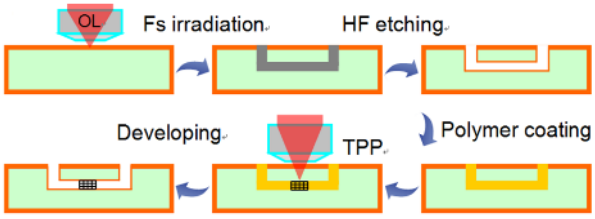

Figure 15: Schematic illustration of the procedure for fabrication of ship-in-a-bottle biochips by the hybrid technique, which mainly involves FLAE of photosensitive glass (femtosecond laser direct writing followed by annealing, HF etching, a second anneal to smooth the inner surfaces), and TPP inside the microfluidic structures formed by FLAE (polymer filling, femtosecond laser direct writing and development) [128].

(Fig. 16(c)) [130]. The fabricated optofluidic device was applied for simultaneous cell detection and counting. The principle of cell detection with the optofluidic device is shown in Fig. 16(d). When the white light is incident from the bottom side of the microchip, the microlens produces a focal spot above the microfluidic channel. If a cell then passes above the microlens, it significantly affects the light

intensity at the focal spot owing to scattering, absorption, and refraction. As a result, the measurement of the time-dependent variation of light intensity at the focal spot enables cell detection. The center-pass unit is composed of an M-shaped confinement wall with 9-μm diameter apertures, which restricts passage of the cells through the edges of two adjacent microlenses for the detection of all cells. In addition, this optofluidics device can also filter out deformed cells. Consequently, coupling-free simultaneous counting of only normal cells with a 100% success rate has been demonstrated.

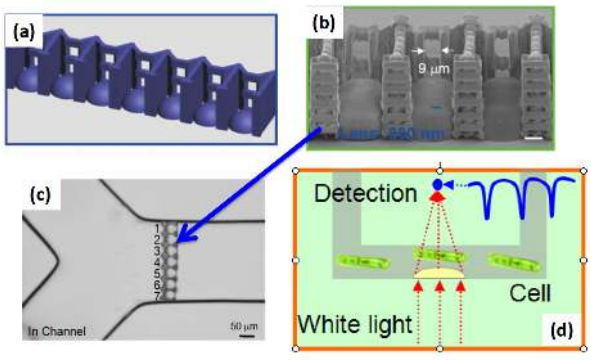

Figure 16: (a) Schematic illustration and (b) SEM image of a microlens array combined with center-pass units formed by TPP. (c) Optical microscope image of 3D glass microfluidic integrated with the microlens array combined with center-pass units. (d) Principle of cell detection with the fabricated optofluidics device [130].

8 Shaped beam processing

Tailoring ultrafast laser pulses is one of the key technologies to enhance the performance of ultrafast laser processing in terms of fabrication efficiency, quality, and resolution [131–134]. Spatial manipulation of laser pulses is effective to increase the fabrication speed, that is, increased throughput by multibeam parallel processing and enhancement of the laser energy utilization efficiency [135–140]. Temporal beam shaping enables the laser energy to be efficiently deposited to the materials, which improves the fabrication quality and resolution. The most typical device used to both temporally and spatially tailor the ultrafast laser beam is an SLM. In addition, spatiotemporal manipulation by the use of optical gratings, in which the wavelength components in the ultrafast laser pulse are spatiotemporally dispersed, offers excellent performance for internal modification and 3D fabrication because of the more spatially localized confinement of multiphoton absorption [141, 142].

8.1 Temporal shaping

Tailored ultrafast laser pulses obtained by shaping an ultrafast laser pulse have the potential to control the transient free-electron density and further excitation, which can improve the fabrication quality, spatial resolution, and/or processing efficiency in the ultrafast laser processing of materials. Shaped ultrafast laser pulses have been demonstrated in the ablation of fused silica and CaF_2. The experimental results revealed that irradiation with a conventional single-pulse train did not produce the best machined surface [131]. In contrast, irradiation with a double- or triple-pulse train with an almost 2-ps pulse separation produced better ablation holes than the single-pulse train. This is considered to be due to transient changes in the material properties that result from swift excitation and charge trapping. The divided energy delivery by multiple pulse irradiation controls the defined electron density and lattice deformation at the surface that follow material softening by the initial pulse, which results in a change in the energy coupling for the subsequent pulses. This permits heating to be controlled, which enables relaxation of the induced stresses and improvement of ablated structures. Similar behavior has also been observed by burst mode irradiation with ultrafast laser pulses (e.g., ca. 400 identical 1 ps pulses with a pulse separation of 7.5 ns), which allowed higher quality ablation with less microcracks and shock-induced effects than a single high-fluence laser pulse [132]. Very smooth holes with diameters of 7–10 μm and depths of ca. 30 μm were produced in fused silica without the formation of fractures, cracks, or surface swelling.

A shaped pulse that resembles temporary asymmetric pulses for which the amplitudes decrease or increase amplitude over time [see Fig. 17(a)] was used for the nanoablation of fused silica [133]. Control of the balance of multiphoton ionization and avalanche ionization enables control of the spatial free-electron density because of the Gaussian beam profile of the laser beam combined with the various intensity-dependent processes. Thus, the fabrication of ca. 100 nm diameter holes was achieved using a 790-nm wavelength ultrafast laser beam with a spot size of 1.4 μm [see Fig. 17(b)].

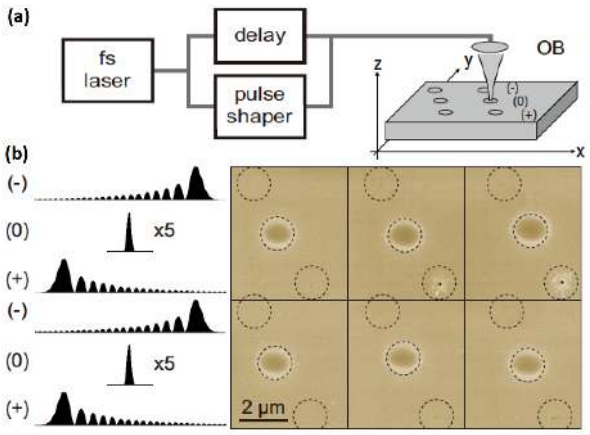

Figure 17: (a) Schematics of experimental setup and fabrication procedure. For material processing, the pulse energy in the x-direction was increased in steps of 6 nJ and the focal z position in the y-direction was changed by 1 µm. For each setting, three laser pulses were applied, all having the same energy: one with negative cubic phase (–), one unshaped (0), and one with positive cubic phase (+) depicted also by the dotted circles in (b), where they indicate diffraction limit. (b) Transient laser intensities and corresponding SEM images of a subset of laser-generated structures in fused silica obtained by the procedure described in (a). Top row: surface in focal plane; lower row: surface 1 µm below focal plane. The large structure (dark color parts) in all areas is due to the unshaped pulses (0) and their size is close to the diffraction limit. The small holes are created for positive cubic phase (+) in the middle and right photos of the top row. In contrast, negative cubic phase, that is, the time reversed pulse, does not induce any visible change [133]. Reproduced with permission from The Optical Society of America, ©2012 by The Optical Society of America.

8.2 Spatial beam shaping

The multiple parallel pulses that result from spatial beam shaping provide an opportunity for ultrafast laser processing to enhance processing throughput and improve energy-use efficiency. Multiple parallel pulses can be generated by either passive optical components such as diffractive optical elements or active components such as an SLM and deformable mirror, the latter of which has an obvious advantage in terms of flexibility.

Multiple optical waveguides have been simultaneously written in glass by direct writing using multiple laser spots generated with an SLM [136]. Different types of bent optical waveguides can be written by continuously changing the positions of the laser spots through the switching of computer-generated holograms (CGHs) because the spatial phase distribution is modulated by the CGH on a liquid–crystal SLM, which is not possible with passive optical components. The multiple parallel pulses generated by an SLM have also been applied to fabricate complex 2D and 3D microstructures, both symmetric and asymmetric, by TPP [138], where each focus spot in the parallel pulses was individually controlled in terms of position and laser intensity. Figure 18 shows a schematic and an SEM image of the parallel fabrication of asymmetric 3D microstructures. Two different 3D polymer structures were simultaneously produced by individual control of two focus spots. It should be noted that this technique is effective at reducing the processing time for the fabrication of complex large-scale structures.

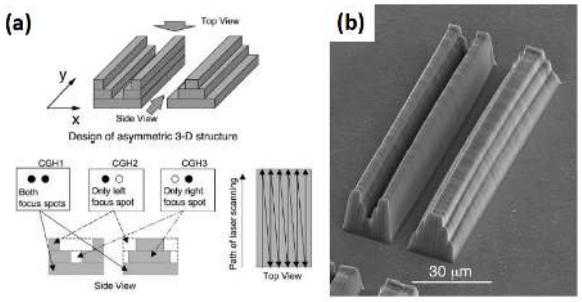

Figure 18: Simultaneous fabrication of asymmetric 3D polymer structures (convex and concave). (a) Design and fabrication protocol. (b) SEM image of structures fabricated by individual control of two focal spots [138]. Reproduced with permission from The Optical Society of America, ©2010 by The Optical Society of America.

Another scheme for spatial beam shaping is high-aspect-ratio nanochannel formation in glass using a non-diffractive femtosecond Bessel pulse [140]. A Bessel beam can be generated by an axicon lens. An SLM is used to imprint the spatial phase of the axicon onto the femtosecond laser beam to generate the femtosecond Bessel pulse. Figure 19 shows an SEM image of a through channel with a diameter of ca. 400 nm formed in 43-µm thick glass (aspect ratio: > 100) by a femtosecond Bessel pulse.

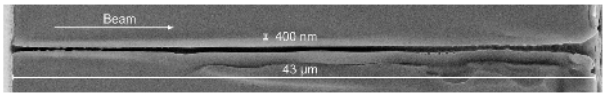

Figure 19: SEM image of a through channel with a diameter of about 400 nm formed in 43-µm thick glass (aspect ratio: > 100) by a femtosecond Bessel pulse [140]. Reproduced with permission from The American Institute of Physics, ©2010 by The American Institute of Physics.

The high peak intensity of ultrafast laser can keep the laser beam focused at a long range because of nonlinear propagation effects without the use of special optics,

which is called self-guiding or filamentation [116, 143]. The peak power of an ultrafast laser can easily reach the critical power required to induce self-focusing by the Kerr effect [144, 145]. Loosely focused ultrafast laser pulses generate a filament with a diameter of approximately 2 μm up to several hundred micrometers in length because of the dynamic balance between self-focusing and self-diffraction by the plasma generated in the filament [146, 147]. Ultrafast laser filamentation produced in transparent materials can be used for fabrication of 3D photonic devices [143, 148, 149], bonding [116], and cutting/drilling [150] of glass and other materials.

8.3 Spatiotemporal beam shaping

Spatiotemporal focusing, which forms an ultrafast pulse only at the focal plane, was originally developed for multiphoton microscopy to improve the signal-to-background ratio [151]. This method was applied to 3D internal processing with an ultrafast laser to improve the depth fabrication resolution (resolution along the laser beam axis) [141]. One of the issues with optical waveguide writing and microfluidic channel formation inside transparent materials using ultrafast lasers is the longitudinally elongated cross-sectional shapes of the formed structures, because of the mismatch between the focal radius and the Rayleigh length. Spatial beam shaping using a narrow slit [152] or a pair of cylindrical lenses [153] was used to achieve balanced transverse and vertical resolutions for the formation of circular cross sections. However, in both the slit and cylindrical lens beam shaping schemes, balanced transverse and vertical resolutions are available only in the 2D plane perpendicular to the translational direction of the sample. Therefore, to write arbitrary 3D structures in transparent materials requires 3D isotropic resolution for the ultimate goal of 3D internal processing with ultrafast lasers. In the spatiotemporal focusing method, the femtosecond laser pulse is first spatially dispersed to elongate the pulse width using a pair of parallel gratings before introduction onto the focal lens, as schematically illustrated in Fig. 20(a) [141]. Temporal focusing is achieved at the focus position because different frequency components spatially overlap only near the focus, so that the original ultrashort pulse width is reproduced to maximize the peak intensity at the focus. This improves the depth resolution in femtosecond laser multiphoton processing because the peak intensity decreases rapidly because of the broadening of the pulse width when the pulse is moving away from the geometric focal spot. Figures 20(c) and 20(g) shows the results of microfluidic channel fabrication with almost circular cross-sections through control of the laser power and the beam diameter incident on the objective lens, regardless of the laser scanning direction.

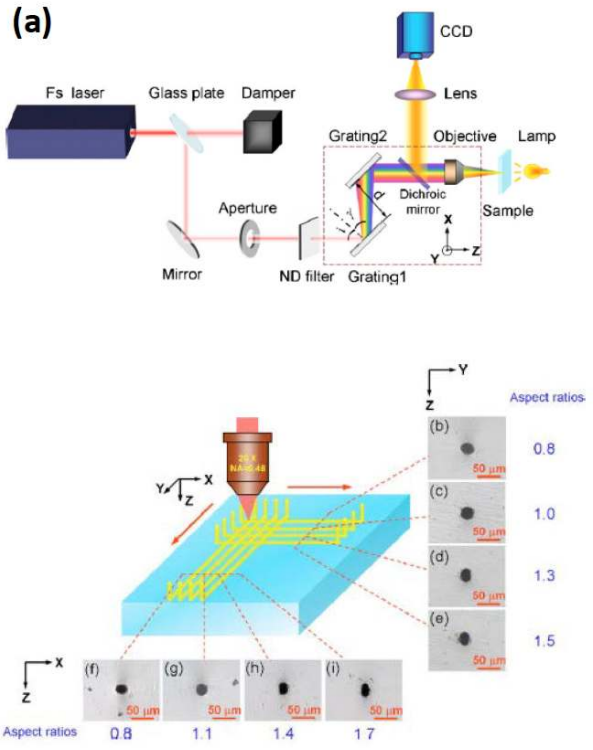

Figure 20: (a) Experimental setup for spatiotemporal focusing of a femtosecond laser beam. (b–i) Optical micrographs of the microfluidic channel cross section. The beam sizes and laser powers are 2 mm and 4 mW in (b) and (f), 3 mm and 3.5 mW in (c) and (g), 4 mm and 2 mW in (d) and (h), and 5 mm and 2 mW in (e) and (i) [141].

As described in Section 8.3, the high peak intensity of ultrafast laser can induce filamentation of laser beam, which frequently results in elongated structures in the internal modification of transparent materials (particularly in highly nonlinear materials such as polymers and crystals). Although the filamentation is beneficial for some applications, it is not preferable for some other applications including waveguide writing and microfluidic channel fabrication. The spatiotemporal focusing method provides the ability to eliminate the filamentation [141, 154].

9 Commercial and industrial applications

The distinctly excellent features of ultrafast laser processing and the development of reliable high-power ultrafast laser systems have pushed this kind of processing method into commercial and industrial applications. Panasonic USA used picosecond lasers for the first time in mass production to produce funnel-shaped ink-jet nozzles. The picosecond laser, together with a PC-controlled scanning mirror, can rapidly fabricate reproducible holes in stainless steel with high precision [155]. As described in Section 3, irradiation by a femtosecond laser in halogen gas ambient produces conical microstructures on an Si surface that can then act as an antireflective surface. This technique was commercialized by SiOnyx Inc for the production of photovoltaic Si solar cells [156]. Average efficiencies as high as 16.9% and a 20% reduction of the Si substrate thickness have led to a 10–15% reduction in costs.

Ultrafast laser micromachining and patterning also offer further applications in the electronics industry. Ultrafast laser micromachining is expected to be used for the manufacture of Si 3D integrated circuits (ICs). The fabrication of current 3D ICs relies on 3D assembly, which electrically connects stacked chips to form a single circuit. A key technology for 3D assembly is the formation of through Si vias (TSVs), which are vertical electrical connections that pass completely through silicon chips to electrically connect vertically assembled Si ICs. Ultrafast laser micromachining is a potential candidate for the rapid formation of high-aspect-ratio TSVs. In addition, ultrafast laser micromachining is used to perform scribing and dicing of very thin glass to hard glass with high-quality edge and flexible geometry and without crack formation. As such, this process has been applied to the mass production of displays for cell phones and tablet computers [157]. Sapphire dicing by ultrafast lasers is an urgent requirement because of an increased demand for sapphire substrates for smart phones. Ultrafast laser scribing and patterning are also reliable for the manufacture of photovoltaic solar cells based on copper indium gallium (di)selenide (CIGS) or organic photovoltaics (OPV) [158]. For CIGS solar cells, ultrafast lasers are used to isolate the back contact (Mo) between cells (P1 process), selectively remove the CIGS layer from the top of the back contact layer (P2 process), and selectively remove the absorber and front contact (transparent conductive oxide) layers (P3 process). Other applications of ultrafast laser patterning include the manufacture of active matrix organic light-emitting diode (AMOLED) displays.

Ultrafast laser processing is also widely used in the automotive and railway industries because of its potential to satisfy many requirements in these fields, including miniaturization, high precision, high quality, applicability to a diversity of materials, variety of variants, smaller lots, and cost-effectiveness [159]. For example, ultrafast lasers have been used to produce exhaust gas sensors made of special ceramic layer systems. Ultrafast laser trimming of sensor elements enables the exhaust gas properties to be measured faster and more precisely. Ultrafast laser microstructuring was used for the fabrication of drainage grooves in the injector of common rail diesel systems, which resulted in a more reliable, powerful, and environment-friendly system.

Another important application of ultrafast laser processing is in the medical field, where it is used for the fabrication of functional medical stents, which are now commercially available. The stent material fabricated by a nanosecond laser is limited to stainless steel; however, the use of ultrafast laser processing extends this to functional materials such as bioresorbable polymers and highly X-ray visible materials [160]. The ultrafast laser is also widely used for medical treatment such as LASIK (laser-assisted in situ keratomileusis), which is a refractive surgery used to correct myopia, hyperopia, and astigmatism. In this treatment, the ultrafast laser is used only for the formation of the corneal flap and subsequent keratomileusis is performed with an excimer laser [161]. Additionally, a femto lamellar keratomileusis, more commonly referred to as small incision lenticule extraction (SMILE), is already clinically available in some regions, which is all-femtosecond laser refractive surgery without creation of flaps [162]. Another medical treatment using ultrafast lasers is treatment for tooth cavities.

10 Summary and future prospects

Ultrafast lasers provide unique advantages in materials processing because of the ultrashort pulse width and extremely high peak intensity that cannot be achieved with existing microfabrication technologies. The advantages include suppression of heat diffusion and the formation of an HAZ, processing of transparent materials by multiphoton absorption, internal modification and 3D processing of transparent materials, and nanofabrication ability. Ultrafast lasers can thus perform high-quality, high-precision surface micromachining of various materials, including metals, semiconductors, ceramics, soft materials (e.g., polymers and biotissues), and even brittle ma-

terials (e.g., glasses). Nano- and microstructured surfaces formed by ultrafast laser irradiation provide unique and useful properties in terms of friction, adhesion, optical absorption, and hydrophobicity. In addition, nanoscale fabrication resolution beyond the diffraction limit is achievable with ultrafast laser processing. The typical fabrication resolution for TPP is ca. 100 nm, which can be further improved to be down to ca. 9 nm when STED is used. Near-field ablation using either nanotips or nanospheres can realize super high resolution, far beyond the diffraction limit, while ablation using a linearly polarized ultrafast laser beam with the intensity carefully reduced to a level very near the ablation threshold results in the fabrication of nanogrooves with widths less than 50 nm by far-field ablation. Internal modification of transparent materials is only available with ultrafast lasers and is thus widely applied to fabricate 3D photonics, data storage, and microfluidic and optofluidic devices. The microwelding of glass substrates is another recent topic in internal modification by ultrafast lasers. Shaping the spatial, temporal, and spatiotemporal profiles of ultrafast laser pulses can enhance the performance of ultrafast laser processing with respect to the improvement in the throughput, energy efficiency, fabrication quality, and fabrication resolution. These unique advantages of ultrafast laser processing have resulted in its emergence in commercial and industrial applications, such as glass dicing for the production of cell phones and tablet computers, scribing and patterning of photovoltaic solar cells, the production of car components in both serial production and racing sports manufacturers, and the fabrication of medical stents. Ultrafast lasers are also practical tools for medical treatment including the refractive surgery and the treatment of teeth cavities.

Although much effort has been made by many researchers to elucidate the detailed mechanisms for the interaction between ultrafast laser irradiation and matter, it has yet to be fully understood. Therefore, research and development continue, which is important not only for pure science but also for the commercialization of ultrafast laser processing. Hybrid techniques of additive, undeformative, and subtractive manufacturing will also provide capabilities in diversifying the geometry and/or increasing the functionalities of fabrication targets, which is expected to further enhance the performance of ultrafast laser processing. Shaped beam processing techniques in spatial, temporal, and spatiotemporal schemes will also contribute to enhanced performance in terms of high quality, high efficiency, and high resolution. Meanwhile, attempts to further improve the fabrication resolution far beyond the diffraction limit will proceed. In particular, the development of techniques to achieve super high resolution in far-field ablation is highly desirable. Although not discussed earlier, ultrafast lasers have the potential for application to the synthesis of new materials because they can generate extremely high temperatures and pressures in materials. For example, femtosecond-laser-driven shock has been used to create the high-pressure ε phase of iron [163]. Microexplosions triggered by femtosecond laser pulses have generated pressures greater than 380 GPa inside sapphire, which resulted in the formation of bcc Al with a crystallite size of ca. 18 ± 2 nm [164]. The unique characteristics of ultrafast laser processing offer the possibility to develop new processes that are unique in the future.

Ultrafast laser processing is already used for some commercial and industrial applications, and this trend is expected to be further accelerated because of the distinct advantage of ultrafast laser processing over conventional laser processing. To this end, the development of high-power, stable, reliable ultrafast laser systems that are reasonably priced is urgently demanded. In addition, the development of killer applications such as printed board drilling by CO_2 lasers and photolithography by excimer lasers is important to establish a firm position for ultrafast laser processing in manufacturing.

References

[1] Sugioka K, Cheng Y. Ultrafast lasers—reliable tools for advanced materials processing. Light Sci. Appl. 2014, 3, e149.
[2] Sugioka K, Cheng Y. Ultrafast laser processing: from micro- to nanoscale. Pan Stanford Publishing, Singapore, 2013.
[3] Momma C, Chichkov BN, Nolte S, von Alvensleben F, Tünnermann A, Welling H, Wellegehausen B. Short-pulse laser ablation of solid targets. Opt. Commun. 1996, 129, 134–142.
[4] Bärsch N, Koörber K, Ostendorf A, Tönshoff KH. Ablation and cutting of planar silicon devices using femtosecond laser pulses. Appl. Phys. A 2003, 77, 237–242.
[5] Küper S, Stuke M. Ablation of polytetrafluoroethylene (Teflon) with femtosecond UV excimer laser pulses. Appl. Phys. Lett. 1989, 54, 4–6.
[6] Krüger J, Kautek W. Femtosecond-pulse visible laser processing of transparent materials. Appl. Surf. Sci. 1996, 96–98, 430–438.
[7] Davis KM, Miura K, Sugimoto N, Hirao K. Writing waveguides in glass with a femtosecond laser. Opt. Lett. 1996, 21, 1729–1731.
[8] Glezer EN, Milosavljevic M, Huang L, Finlay RJ, Her TH, Callan JP, Mazur E. Three-dimensional optical storage inside transparent materials. Opt. Lett. 1996, 21, 2023–2025.
[9] Sugioka K, Cheng Y. Femtosecond laser three-dimensional micro- and nanofabrication. Appl. Phys. Rev. 2014, 1, 041303.
[10] Srinivasan R, Sutcliffe E, Braren B. Ablation and etching of polymethylmethacrylate by very short (160 fs) ultraviolet (308 nm)

laser pulses. Appl. Phys. Lett. 1987, 51, 1285–1287.
[11] Küper S, Stuke M. Femtosecond UV excimer laser ablation. Appl. Phys. B 1987, 44, 199–204.
[12] Squier J, Salin F, Mourou G, Harter D. 100-fs pulse generation and amplification in Ti:Al_2O_3. Opt. Lett. 1991, 16, 324–326.
[13] Rudd, JV, Korn G, Kane S, Squier J, Mourou G, Bado P. Chirped-pulse amplification of 55-fs pulses at a 1-kHz repetition rate in a Ti:Al_2O_3 regenerative amplifier. Opt. Lett. 1993, 18, 2044–2046.
[14] Maruo S, Nakamura O, Kawata S. Three-dimensional microfabrication with two-photon-absorbed photopolymerization. Opt. Lett. 1997, 22, 132–134.
[15] Hashida M, Fujita M, Tsukamoto M, Semerok AF. Femtosecond laser ablation of metals: precise measurement and analytical model for crater profiles. Proc. SPIE 2003, 4830, 452–457.
[16] Costache F, Henyk M, Reif J. Surface patterning on insulators upon femtosecond laser ablation. Appl. Surf. Sci. 2003, 208–209, 486–491.
[17] Borowiec A, Haugen HK. Subwavelength ripple formation on the surfaces of compound semiconductors irradiated with femtosecond laser pulses. Appl. Phys. Lett. 2003, 82, 4462–4464.
[18] Atanasov PA, Takada H, Nedyalkov NN, Obara M. Nanohole processing on silicon substrate by femtosecond laser pulse with localized surface plasmon polariton. Appl. Surf. Sci. 2007, 253, 8304–8308.
[19] Eversole D, Luk'yanchuk B, Ben-Yakar A. Plasmonic laser nanoablation of silicon by the scattering of femtosecond pulses near gold nanospheres. Appl. Phys. A 2007, 89, 283–291.
[20] Arai A, Bovatsek J, Yoshino F, Liu Z, Cho GC, Shah L, Fermann ME, Uehara Y. Fiber chirped pulse amplification system for micromachining. Proc. SPIE 2006, 6343, 63430S.
[21] Kleinbauer J, Eckert D, Weiler S, Sutter DH. 80 W ultrafast CPA-free disk laser. Proc. SPIE 2008, 6871, 68711B.
[22] Marchese SV, Baer CRE, Engqvist AG, Hashimoto S, Maas DJ, Golling M, Suedmeyer T, Keller U. Femtosecond thin disk laser oscillator with pulse energy beyond the 10-microjoule level. Opt. Express 2008, 16, 6397–6407.
[23] Rizvi NH, Femtosecond laser micromachining: current status and applications. RIKEN Review 2003, 50, 107–112.
[24] Birnbaum M, Semiconductor surface damage produced by ruby lasers. J. Appl. Phys. 1965, 36, 3688–3689.
[25] Emmony DC, Howson RP, Willis LJ. Laser mirror damage in germanium at 10.6 μm. Appl. Phys. Lett. 1973, 23, 598–600.
[26] Sakabe S, Hashida M, Tokita S, Namba S, Okamuro K. Mechanism for self-formation of periodic grating structures on a metal surface by a femtosecond laser pulse. Phys. Rev. B 2009, 79, 033409.
[27] Miyaji G, Miyazaki K. Ultrafast dynamics of periodic nanostructure formation on diamond-like carbon films irradiated with femtosecond laser pulses. Appl. Phys. Lett. 2006, 89, 191902.
[28] Reif J, Costache F, Henyk M, Pandelov SV. Ripples revisited: non-classical morphology at the bottom of femtosecond laser ablation craters in transparent dielectrics. Appl. Surf. Sci. 2002, 197–198, 891–895.
[29] Wang C, Huo H, Johnson M, Shen M, Mazur E. The thresholds of surface nano-/micromorphology modifications with femtosecond laser pulse irradiations. Nanotechnology 2010, 21, 075304.
[30] Bhardwaj VR, Simova E, Rajeev PP, Hnatovsky C, Taylor RS, Rayner DM, Corkum PB. Optically produced arrays of planar nanostructures inside fused silica. Phys. Rev. Lett. 2006, 96, 057404.
[31] Miyaji G, Miyazaki K. Origin of periodicity in nanostructuring on thin film surfaces ablated with femtosecond laser pulses. Opt. Express 2008, 16, 16265–16271.
[32] Dusser B, Sagan. Z, Soder H, Faure N, Colombier JP, Jourlin M, Audouard E. Controlled nanostructures formation by ultra fast laser pulses for color marking. Opt. Express 2010, 18, 2913–2924.
[33] Vorobyev AY, Guo C. Colorizing metals with femtosecond laser pulses. Appl. Phys. Lett. 2008, 92, 041914.
[34] Lochbihler H. Colored images generated by metallic subwavelength gratings. Opt. Express 2009, 17, 12189–12196.
[35] Her TH, Finlay RJ, Wu C, Deliwala S, Mazur E. Microstructuring of silicon with femtosecond laser pulses. Appl. Phys. Lett. 1998, 73, 1673–1675.
[36] Her TH, Finlay RJ, Wu C, Mazur E. Femtosecond laser-induced formation of spikes on silicon. Appl. Phys. A 2000, 70, 383–385.
[37] Carey JE, Crouch CH, Shen M, Mazur E. Visible and near-infrared responsivity of femtosecond-laser microstructured silicon photodiodes. Opt. Lett. 2005, 30, 1773–1775.
[38] Younkin R, Carey JE, Mazur E, Levinson JA. Friend CM. Infrared absorption by conical silicon microstructures made in a variety of background gases using femtosecond laser pulses. J. Appl. Phys. 2003, 93, 2626–2629.
[39] Wang F, Chen C, He H, Liu S. Analysis of sunlight loss for femtosecond laser microstructured silicon and its solar cell efficiency. Appl. Phys. A 2011, 103, 977–982.
[40] Nayak BK, Gupta M, Kolasinski K. Spontaneous formation of nanospiked microstructures in germanium by femtosecond laser irradiation. Nanotechnology 2007 18, 195302.
[41] Nayak BK, Gupta M. Self-organized micro/nano structures in metal surfaces by ultrafast laser irradiation. Optics and Lasers in Engineering 2010, 48, 940–949
[42] Dolgaev SI, Lavrishev SV, Lyalin AA, Simakin AV, Voronov VV, Shafeev GA. Formation of conical microstructures upon laser evaporation of solids. Appl. Phys. A 2001, 73, 177–181.
[43] Chiba T, Komura R, Mori A. Formation of Micropeak Array on a Silicon Wafer, Jpn. J. Appl. Phys. 2000, 39, 4803–4810.
[44] Zorba V, Stratakis E, Barberoglou M, Spanakis E, Tzanetakis P, Anastasiadis SP, Fotakis C. Biomimetic artificial surfaces quantitatively reproduce the water repellency of a lotus leaf. Adv. Mater. 2008, 20, 4049–4054.
[45] Kawata S, Sun HB, Tanaka T, Takada K. Finer features for functional microdevices. Nature 2001, 412, 697–698.
[46] Nakashima S, Sugioka K, Midorikawa K. Enhancement of resolution and quality of nano-hole structure on GaN substrates using the second-harmonic beam of near-infrared femtosecond laser. Appl. Phys. A 2010, 101, 475–481.
[47] Nakashima S, Sugioka K, Ito T, Takai H, Midorikawa K. Fabrication of high-aspect-ratio nanohole arrays on GaN surface by using wet-chemical-assisted femtosecond laser ablation. J. Laser Micro/Nanoeng. 2011, 6, 15–19.
[48] Chong TC, Hong MH, Shi LP. Laser precision engineering: from microfabrication to nanoprocessing. Laser Photonics Rev. 2010, 4,123–143.
[49] Chimmalgi A, Choi TY, Grigoropoulos CP, Komvopoulos K. Femtosecond laser aperturelessnear-field nanomachining of metals assisted by scanning probe microscopy. Appl. Phys. Lett. 2003, 82, 1146–1148.

[50] Korte F, Nolte S, Chichkov BN, Bauer T, Kamlage G, Wagner T, Fallnich C, Welling H. Far-field and near-field material processing with femtosecond laser pulses. Appl. Phys, A 1999, 69, S7–S–11.
[51] Tanaka Y, Obara G, Zenidaka A, Terakawa M, Obara M. Femtosecond laser near-field nanoablation patterning using Mie resonance high dielectric constant particle with small size parameter. Appl. Phys. Lett. 2010, 96, 261103.
[52] Eversole D, Luk'yanchuk B, Ben-yakar A. Plasmonic laser nanoablation of silicon by the scattering of femtosecond pulses near gold nanospheres. Appl. Phys. A 2007, 89, 283–291.
[53] Liao Y, Shen YL, Qiao LL, Chen D, Cheng Y, Sugioka K, Midorikawa, K. Femtosecond laser nanostructuring in porous glass with sub-50 nm feature sizes. Opt. Lett. 2013, 38, 187–189.
[54] Liao Y, Cheng Y, Liu CN, Song JX, He F, Shen Y, Chen D, Xu Z, Fan Z, We Xi, Sugioka K, Midorikawa K. Direct laser writing of sub-50 nm nanofluidic channels buried in glass for three-dimensional micro-nanofluidic integration. Lab Chip 2013, 13, 1626–1631.
[55] Buividas R, Rekštytė S, Malinauskas M, Juodkazis S. Nanogroove and 3D fabrication by controlled avalanche using femtosecond laser pulses. Opt. Mater. Express 2013, 3, 1674–1686.
[56] Liu J, Jia T, Zhou K, Feng D, Zhang S, Zhang H, Jia X, Sun Z, Qiu J. Direct writing of 150 nm gratings and squares on ZnO crystal in water by using 800 nm femtosecond laser. Opt. Express 2014, 22, 32361–32370.
[57] Shimotsuma Y, Kazansky PG, Qiu JR, Hirao K. Self-organized nanogratings in glass irradiated by ultrashort light pulses. Phys. Rev. Lett. 2003, 91, 247405.
[58] Cumpston BH, Ananthavel SP, Barlow S, Dyer DL, Ehrlich JE, Erskine LL, Heikal AA, Kuebler SM, Lee IYS, McCord-Maughon D, Qin JQ, Rockel H, Rumi M, Wu XL, Marder SR, Perry JW. Two-photon polymerization initiators for three-dimensional optical data storage and microfabrication. Nature 1999, 398, 51–54.
[59] Zhou WH, Kuebler SM, Braun KL, Yu TY, Cammack JK, Ober CK, Perry, JW, Marder SR. An efficient two-photon-generated photoacid applied to positive-tone 3D microfabrication. Science 2002, 296, 1106–1109.
[60] Tan DF, Li Y, Qi FJ, Yang H, Gong QH, Dong XZ, Duan XM. Reduction in feature size of two-photon polymerization using SCR500. Appl. Phys. Lett. 2007, 90, 071106.
[61] Hell SW, Wichmann J. Breaking the diffraction resolution limit by stimulated emission: stimulated-emission-depletion fluorescence microscopy. Opt. Lett. 1994, 19, 780–782.
[62] Li L, Gattass RR, Gershgoren E, Hwang H, Fourkas JT. Achieving l/20 resolution by one-color initiation and deactivation of polymerization. Science 2009, 324, 910–913.
[63] Gan Z, Cao Y, Evans RA, Min Gu. Three-dimensional deep sub-diffraction optical beam lithography with 9 nm feature size. Nat. Comm. 2013, 4, 2061.
[64] Guo R, Xiao S, Zhai X, Li J, Xia A, Huang W. Micro lens fabrication by means of femtosecond two photon photopolymerization. Opt. Express 2006, 14, 810–816.
[65] Sun HB, Matsuo S, Misawa H. Three-dimensional photonic crystal structures achieved with two-photon-absorption photopolymerization of resin. Appl. Phys. Lett. 1999, 74, 786–788.
[66] Seet KK, Mizeikis V, Matsuo S, Juodkazis S, Misawa H. Three-dimensional spiral- architecture photonic crystals obtained by direct laser writing. Adv. Mater. 2005, 17, 541–545.
[67] Maruo S, Inoue H. Optically driven micropump produced by three-dimensional two-photon microfabrication. Appl. Phys. Lett. 2006, 89, 144101.
[68] Maruo S, Inoue H. Optically driven viscous micropump using a rotating microdisk, Appl. Phys. Lett. 2007, 91, 084101.
[69] Tian Y, Zhang YL, Ku JF, He Y, Xu BB, Chen QD, Xia H, Sun HB. High performance magnetically controllable microturbines. Lab Chip 2010, 10, 2902–2905.
[70] Wang J, He Y, Xia H, Niu LG, Zhang R, Chen QD, Zhang YL, Li YF, Zeng SJ, Qin JH, Lin BC, Sun HB. Embellishment of microfluidic devices via femtosecond laser micronanofabrication for chip functionalization. Lab Chip 2010, 10, 1993–1996.
[71] Wu D, Chen QD, Niu LG, Wang JN, Wang J, Wang R, Xia H, Sun HB. Femtosecond laser rapid prototyping of nanoshells and suspending components towards microfluidic devices. Lab Chip 2009, 9, 2391–2394.
[72] Lim TW, Son Y, Jeong YJ, Yang DY, Kong HJ, Lee KS, Kim DP. Three-dimensionally crossing manifold micro-mixer for fast mixing in a short channel length. Lab Chip 2011, 11,100–103.
[73] Farsari M, Chichkov B. Two-photon fabrication. Nat. Photonics 2009, 3, 450–452.
[74] Ovsianikov A, Malinauskas M, Schlie S, Chichkov B, Gittard S, Narayan R, Löblerc M, Sternbergc K, Schmitzc KP, Haverich A. Three-dimensional laser micro- and nano-structuring of acrylated poly(ethylene glycol) materials and evaluation of their cytotoxicity for tissue engineering applications. Acta Biomaterialia 2011, 7, 967–974.
[75] Tayalia P, Mendonca CR, Baldacchini T, Mooney DJ, Mazur E. 3D cell-migration studies using two-photon engineered polymer scaffolds. Adv. Mater. 2008, 20, 4494–4498.
[76] Sun ZB, Dong XZ, Chen WQ, Nakanishi S, Duan XM, Kawata, S. Multicolor polymer nanocomposites: In situ synthesis and fabrication of 3D microstructures. Adv. Mater. 2008, 20, 914–919.
[77] Xia H, Wang J, Tian Y, Chen QD, Du XB, Zhang YL, He Y, Sun HB. Ferrofluids for fabrication of remotely controllable micro-nanomachines by two-photon polymerization. Adv. Mater. 2010, 22, 3204–3207.
[78] Ushiba S, Shoji S, Masui K, Kono J, Kawata S. Direct laser writing of 3D architectures of aligned carbon nanotubes. Adv. Mater. 2014, 26, 5653–5657.
[79] Miura K, Qiu J, Fujiwara S, Sakaguchi S, Hirao K. Three-dimensional optical memory with rewriteable and ultrahigh density using the valence-state change of samarium ions.Appl. Phys. Lett. 2002, 80, 2263–2265.
[80] Luo FF, Qian B, Lin G, Xu J, Liao Y, Song J, Sun HY, Zhu B, Qiu JR, Zhao QZ, Xu Z. Redistribution of elements in glass induced by a high-repetition-rate femtosecond laser. Opt. Express 2010, 18, 6262–6269.
[81] Hongo T, Sugioka K, Niino H, Cheng Y, Masuda M, Miyamoto I, Takai H, Midorikawa K. Investigation of photoreaction mechanism of photosensitive glass by femtosecond laser. J. Appl. Phys. 2005, 97, 063517.
[82] Miura K, Shimotsuma Y, Sakakura M, Kanehira S, Hamabe M, Hirao K. Three-dimensional deposition of silicon from silicate glass with dispersed metallic aluminum by a femtosecond laser. Proc. SPIE, 2006, 6413, 64130K.
[83] Marcinkevičius A, Juodkazis S, Watanabe M, Miwa M, Matsuo S, Misawa H, Nishii J. Femtosecond laser-assisted three-dimensional microfabrication in silica. Opt. Lett. 2001, 26, 277–279.

[84] Watanabe W, Asano T, Yamada K, Itoh K, Nishii J. Wavelength division with three-dimensional couplers fabricated by filamentation of femtosecond laser pulses. Opt. Lett. 2003, 28, 2491–2493.

[85] Florea C, Winick KA. Fabrication and characterization of photonic devices directly written in glass using femtosecond laser pulses, J. Lightwave Technol. 2003, 21, 246–253.

[86] Bricchi E, Mills JD, Kazamsky PG, Klappauf BG, Baumberg JJ. Birefringent Fresnel zone plates in silica fabricated by femtosecond laser machining, Opt. Lett. 2002, 27, 2200–2202.

[87] Liao Y, Xu J, Cheng Y, Zhou ZH, He F, Sun H, Song J, Wang X, Xu Z, Sugioka K, Midorikawa K. Electro-optic integration of embedded electrodes and waveguides in $LiNbO_3$ using a femtosecond laser. Opt. Lett. 2008, 33, 2281–2283.

[88] Vella GD, Taccheo S, Osellame R, Festa A, Cerullo G, Laporta P. 1.5 μm single longitudinal mode waveguide laser fabricated by femtosecond laser writing. Opt. Express 2007, 15, 3190–3194.

[89] Kawamura K, Hirano M, Kurobori T, Takamizu D, Kamiya T, Hosono H. Femtosecond-laser-encoded distributed-feedback color center laser in lithium fluoride single crystals. Appl. Phys. Lett. 2004, 84, 311–313.

[90] Osellame R, Hoekstra HJ, Cerullo G, Pollnau M. Femtosecond laser microstructuring:
an enabling tool for optofluidic lab-on-chips. Laser Photonics Rev. 2011, 5, 442–463.

[91] Chaboyer Z, Meany T, Helt LG, Withford MJ, Steel MJ. Tunable quantum interference in a 3D integrated circuit. Sci. Rep. 2015, 5, 9601.

[92] Crespi A, Osellame R, Ramponi R, Brod DJ, Galvão EF, Spagnolo N, Vitelli C, Maiorino E, Mataloni P, Sciarrino F. Integrated multimode interferometers with arbitrary designs for photonic boson sampling. Nat. Photonics 2013, 7, 545–549.

[93] Crespi A, Osellame R, Ramponi R, Giovannetti V, Fazio R, Sansoni L, De Nicola F, Sciarrino F, Mataloni P. Anderson localization of entangled photons in an integrated quantum walk. Nat. Photonics 2013, 7, 322–328.

[94] Watanabe T, Shiozawa M, Tatsu E, Kimura S, Umeda M, Mine T, Shimotsuma Y, Sakakura M, Nakabayashi M, Miura K, Watanabe K. A driveless read system for permanently recorded data in fused silica. Jpn. J. Appl. Phys. 2013, 52, 09LA02.

[95] Zhang JY, Gecevičius M, Beresna M, Kazansky PG. Seemingly unlimited lifetime data storage in nanostructured glass. Phys. Rev. Lett. 2014, 112, 033901.

[96] Masuda M, Sugioka K, Cheng Y, Aoki N, Kawachi M, Shihoyama K, Toyoda K, Helvajian H, Midorikawa K. 3-D microstructuring inside photosensitive glass by femtosecond laser excitation. Appl. Phys. A 2003, 76, 857–860.

[97] Li Y, Itoh K, Watanabe W, Yamada K, Kuroda D, Nishii J, Jiang YY. Three-dimensional hole drilling of silica glass from the rear surface with femtosecond laser pulses. Opt. Lett. 2001, 26, 1912–1914.

[98] Sugioka K, Cheng Y, Midorikawa K. Three-dimensional micromachining of glass using femtosecond laser for lab-on-a-chip device manufacture. Appl. Phys. A 2005, 81, 1–10.

[99] Sugioka K, Hanada Y, Midorikawa K. Three-dimensional femtosecond laser micromachining of photosensitive glass for biomicrochips. Laser Photonics Rev. 2010, 3, 386–400.

[100] Bellouard Y, Said A, Dugan M, Bado P. Fabrication of high-aspect ratio, micro-fluidic channels and tunnels using femtosecond laser pulses and chemical etching. Opt. Express 2004, 12, 2120–2129.

[101] Cheng Y, Sugioka K, Midorikawa K, Masuda M, Toyoda K, Kawachi M, Shihoyama K. Three-dimensional micro-optical components embedded in photosensitive glass by a femtosecond laser. Opt. Lett. 2003, 28, 1144–1146.

[102] Masuda M, Sugioka K, Cheng Y, Hongo T, Shihoyama K, Taka H, Miyamoto I, Midorikawa K. Direct fabrication of freely movable microplate inside photosensitive glass by femtosecond laser for lab-on-chip application. Appl. Phys. A 2004, 78, 1029–1032.

[103] Sugioka K, Cheng Y. Fabrication of 3D microfluidic structures inside glass by femtosecond laser micromachining. Appl. Phys. A, 2014, 114, 215–221.

[104] Ke K, Hasselbrink EF, Hunt A. Rapidly prototyped three-dimensional nanofluidic channel networks in glass substrates. Anal. Chem. 2005, 77, 5083–5088.

[105] Liao Y, Song J, Li E, Luo Y, Shen YL, Chen DP, Cheng Y, Xu ZZ, Sugioka K, Midorikawa K. Rapid prototyping of three-dimensional microfluidic mixers in glass by femtosecond laser direct writing. Lab Chip 2012, 12, 746–749.

[106] Hanada Y, Sugioka K, Shihira-Ishikawa I, Kawano H, Miyawaki A, Midorikawa K. 3D microfluidic chips with integrated functional microelements fabricated by a femtosecond laser for studying the gliding mechanism of cyanobacteria. Lab Chip 2011, 11, 2109–2115.

[107] Crespi A, Gu Y, Ngamsom B, Hoekstra HJ, Dongre C, Pollnau M, Ramponi R, van den Vlekkert HH, Watts P, Cerullo G, Osellame R. Three-dimensional Mach–Zehnder interferometer in a microfluidic chip for spatially-resolved label-free detection. Lab Chip 2010, 10, 1167–1173.

[108] Hanada Y, Sugioka K, Midorikawa K. Highly sensitive optofluidic chips for biochemical liquid assay fabricated by 3D femtosecond laser micromachining followed by polymer coating. Lab Chip 2012, 12, 3688–3693.

[109] Kim M, Hwang DJ, Hiromatsu K, Grigoropoulos CP. Single cell detection using a glass-based optofluidic device fabricated by femtosecond laser pulses. Lab Chip 2009, 9, 311–318.

[110] Schaap A, Rohrlack T, Bellouard Y, Lab on a chip technologies for algae detection: a review. J. Biophotonics 2012, 5, 661–672.

[111] Bragheri F, Minzioni P, Vazquez RM, Bellini N, Paie P, Mondello C, Ramponi R, Cristiani I, Osellame R. Optofluidic integrated cell sorter fabricated by femtosecond lasers. Lab Chip 2012, 12, 3779–3784.

[112] Xu J, Wu D, Hanada Y, Chen C, Wu S, Cheng Y, Sugioka K, Midorikawa K. Electrofluidics fabricated by space-selective metallization in glass microfluidic structures using femtosecond laser direct writing. Lab Chip 2013, 13, 4608–4616.

[113] Xu J, Wu D, Ip JY, Midorikawa K, Sugioka K. Vertical sidewall electrodes monolithically integrated into 3D glass microfluidic chips using water-assisted femtosecond-laser fabrication for in situ control of electrotaxis. RSC Adv. 2015, 5, 24072–24080.

[114] Tamaki T, Watanabe W, Itoh K. Welding of transparent materials using femtosecond laser pulses. Jpn. J. Appl. Phys. 2005, 44, L20–L23.

[115] Zimmermann F, Richter S, Doring S, Tunnermann A, Nolte S. Ultrastable bonding of glass with femtosecond laser bursts. Appl. Opt. 2013, 52, 1149–1154.

[116] Helie D, Lacroix F, Vallee R. Reinforcing a direct bond between optical materials by filamentation based femtosecond laser welding. J. Laser Micro/Nanoeng. 2012, 7, 284–292.

[117] Miyamoto I, Horn A, Göttemann J, Wortmann D, Yoshino F. Fusion welding of glass using femtosecond laser pulses with high-repetition rates. J. Laser Micro/Nanoeng. 2007, 2, 7–14.
[118] Cvecek K, Miyamoto I, Strauss J, Wolf M, Frick T, Schmidt M. Sample preparation method for glass welding by ultrashort laser pulses yields higher seam strength. Appl. Opt. 2011, 50, 1941–1944.
[119] Alexeev I, Cvecek K, Schmidt C, Miyamoto I, Frick T, Schmidt M. Characterization of Shear Strength and Bonding Energy of Laser Produced Welding Seams in Glass. J. Laser Micro/Nanoeng. 2012, 7, 279–283.
[120] Tamaki T, Watanabe W, Itoh K. Laser micro-welding of transparent materials by a localized heat accumulation effect using a femtosecond fiber laser at 1558 nm. Opt. Express 2006, 14, 10460–10468.
[121] Sugioka K, Iida M, Takai H, Midorikawa K. Efficient microwelding of glass substrates by ultrafast laser irradiation using a double-pulse train. Opt. Lett. 2011, 36, 2734–2736.
[122] Okamoto Y, Miyamoto I, Cvecek K, Okada A, Takahashi K, Schmidt M. Evaluation of Molten Zone in Micro-welding of Glass by Picosecond Pulsed Laser. J. Laser Micro/Nanoeng. 2013, 8, 65–69.
[123] Helie D, Gouin S, Vallee R. Assembling an endcap to optical fibers by femtosecond laser welding and milling. Opt. Mater. Express 2013, 3, 1755–1768.
[124] Ratautas K, Raciukaitis G, Gedvilas M. Sphere-to-plate glass welding using picosecond-laser radiation. J. Laser Micro/Nanoeng. 20123, 8, 175–182.
[125] Horn A, Mingareev I, Werth A, Kachel M, Brenk U. Investigations on ultrafast welding of glass-glass and glass-silicon. Appl. Phys. A, 2008, 93, 171–175.
[126] Ozeki Y, Inoue T, Tamaki T, Yamaguchi H, Onda S, Watanabe W, Sano T, Nishiuchi S, Hirose A, Itoh K. Direct welding between copper and glass substrates with femtosecond laser pulses. Appl. Phys. Express 2008, 1, 082601.
[127] Xiong W, Zhou YS, He XN, Gao Y, Mahjouri-Samani M, Jiang L, Baldacchini T, Lu YF. Simultaneous additive and subtractive three-dimensional nanofabrication using integrated two-photon polymerization and multiphoton ablation. Light Sci. Appl. 2012, 1, e6.
[128] Wu D, Wu S, Xu J, Niu L, Midorikawa K, Sugioka K. Hybrid femtosecond laser microfabrication to achieve true 3D glass/polymer composite biochips with multiscale features and high performance: the concept of ship-in-a-bottle biochip. Laser Photonics Rev. 2014, 8, 458–467.
[129] Wu D, Xu J, Niu L, Wu S, Midorikawa K, Sugioka K. In-channel integration of designable microoptical devices using flat scaffold-supported femtosecond-laser microfabrication for coupling-free optofluidic cell counting. Light Sci. Appl. 2015, 4, e228.
[130] Wu D, Niu L, Wu S, Xu J, Midorikawa K, Sugioka K. Ship-in-a-bottle femtosecond laser integration of optofluidic microlens arrays with center-pass units enabling coupling-free parallel cell counting with 100% success rate. Lab Chip 2015, 15, 1515–1523.
[131] Stoian R, Boyle M, Thoss A, Rosenfeld A, Korn G, Hertel IV, Campbell EEB. Laser ablation of dielectrics with temporally shaped femtosecond pulses. Appl. Phys. Lett. 2002, 80, 353–355.
[132] Lapczyna M, Chen KP, Herman PR, Tan HW, Marjoribanks RS. Ultra high repetition rate (133 MHz) laser ablation of aluminum with 1.2-ps pulses. Appl. Phys. A, 1999, 69, S883–S886.
[133] Englert L, Rethfeld B, Haag L, Wollenhaupt M, Sarpe-Tudoran C, Baumert T. Control of ionization processes in high band gap materials via tailored femtosecond pulses. Opt. Express 2007, 15, 17855.
[134] Englert L, Wollenhaupt M, Haag L, Sarpe-Tudoran C, Rethfeld B, Baumert T. Material processing of dielectrics with temporally asymmetric shaped femtosecond laser pulses on the nanometer scale. Appl. Phys. A 2008, 92, 749–753.
[135] Hayasaki Y, Sugimoto T, Takita A, Nishida N. Variable holographic femtosecond laser processing by use of a spatial light modulator. Appl. Phys. Lett. 2005, 87, 0311101.
[136] Sakakura M, Sawano T, Shimotsuma Y, Miura K, Hirao K. Parallel Drawing of Multiple Bent Optical Waveguides Using a Spatial Light Modulator. Jpn. J. Appl. Phys. 2009, 48, 126507.
[137] Sakakura M, Sawano T, Shimotsuma Y, Miura K, Hirao K. Fabrication of three-dimensional 1x4 splitter waveguides inside a glass substrate with spatially phase modulated laser beam. Opt. Express 2010. 18, 12136–12143.
[138] Obata K, Koch J, Hinze U, Chichkov BN. Multi-focus two-photon polymerization technique based on individually controlled phase modulation. Opt. Express 2010, 18, 17193–17200.
[139] Bhuyan MK, Courvoisier F, Lacourt PA, Jacquot M, Furfaro L, Withford MJ, Dudley JM. High aspect ratio taper-free microchannel fabrication using femtosecond Bessel beams. Opt. Express 2010, 18, 566–574.
[140] Bhuyan MK, Courvoisier F, Lacourt PA, Jacquot M, Salut R, Furfaro L, Dudley JM. High aspect ratio nanochannel machining using single shot femtosecond Bessel beams. Appl. Phys. Lett. 2010, 97, 081102.
[141] He F, Xu H, Cheng Y, Ni J, Xiong H, Xu Z, Sugioka K, Midorikawa K. Fabrication of microfluidic channels with a circular cross section using spatiotemporally focused femtosecond laser pulses. Opt. Lett. 2010, 35, 1106–1108.
[142] Vitek DN, Adams DE, Johnson A, Tsai PS, Backus S, Durfee CG, Kleinfeld D, Squier JA. Temporally focused femtosecond laser pulses for low numerical aperture micromachining through optically transparent materials. Opt. Express 2010, 18, 18086–18094.
[143] Itoh K. Ultrafast laser processing of glass. J. Laser Micro/Nanoengin. 2014, 9, 187–191.
[144] Couairon A, Mysyrowicz A. Femtosecond filamentation in transparent media. Phys. Rep. 2007, 441, 47–189.
[145] Chin SL, Hosseini SA, Liu W, Luo Q, Theberge F, Akozbek N, Becker A, Kandidov VP, Kosareva OG, Schroeder H. The propagation of powerful femtosecond laser pulses in optical media: physics, applications, and new challenges. Can. J. Phys. 2005, 83, 863–905.
[146] Cho SH, Kumagai H, Yokota I, Midorikawa K, Obara M. Observation of self-channeled plasma formation and bulk modification in optical fibers using high-intensity femtosecond laser. Jpn. J. Appl. Phys. 1998, 37, L737–L739.
[147] Yamada K, Watanabe W, Toma T, Itoh K, Nishii J. In situ observation of photoinduced refractive-index changes in filaments formed in glasses by femtosecond laser pulses. Opt. Lett. 2001, 6, 19–21.
[148] Yamada K, Watanabe W, Kintaka, K, Nishii J, Itoh K. Volume grating induced by a self-trapped long filament of femtosecond laser pulses in silica glass. J. Appl. Phys. 2003, 42, 6916–6919.

[149] Li YD, Watanabe W, Tamaki T, Nishii J, Itoh, K. Fabrication of Dammann gratings in silica glass using a filament of femtosecond laser. Jpn. J. Appl. Phys. 2005, 44, 5014–5016.
[150] Butkus S, Paipulas D, Sirutkaitis R, Gaizauskas E, Sirutkaitis V. Rapid cutting and drilling of transparent materials via femtosecond laser filamentation. J. Laser Micro/Nanoengin. 2014, 9, 213–220.
[151] Zhu G, van Howe J, Durst M, Zipfel W, Xu C. Simultaneous spatial and temporal focusing of femtosecond pulses. Opt. Express 2005, 13, 2153–2159.
[152] Cheng Y, Sugioka K, Midorikawa K, Masuda M, Toyoda K, Kawachi M, Shihoyama K. Control of the cross-sectional shape of a hollow microchannel embedded in photostructurable glass by use of a femtosecond laser. Opt. Lett. 2003, 28, 55–57.
[153] Cerullo G, Osellame R, Taccheo S, Marangoni M, Polli D, Ramponi R, Laporta P, De Silvestri S. Femtosecond micromachining of symmetric waveguides at 1.5 μm by astigmatic beam focusing. Opt. Lett. 2003, 27, 1938–1940.
[154] Zeng B, Chu W, Gao H, Liu W, Li G, Zhang H, Yao J, Ni J, Chin SL, Cheng Y, Xu Z. Enhancement of peak intensity in a filament core with spatiotemporally focused femtosecond laser pulses. 2011, Phys. Rev. A 84, 063819.
[155] Sugioka K, Gu B, Holmes A. The state of the art and future prospects for laser direct write for industrial and commercial applications. MRS Bull. 2007, 32, 47–54.
[156] SiOnyx solar achieves record results for black silicon solar cells: http://sionyx.com/2011/10/sionyx-solar-achieves-record-results-for-black-silicon-solar-cells-2/.
[157] Weiler S. High-power pico- and femtosecond lasers enable new applications. Laser Focus World 2011, 47, 55–63.
[158] Booth H. Laser processing in industrial solar module manufacturing. J. Laser Micro/Nanoeng. 2010, 5, 183–191.
[159] Bauer Th, König J. Applications and perspectives of ultrashort pulsed lasers. Tech. Dig. LPM 2010, 2010, 127.
[160] Tönshoff HK, Ostendorf A, Nolte S, Korte F, Bauer T. Micromachining using femtosecond lasers. Proc. SPIE 2000, 4088, 136–139.
[161] IntraLaseTM FS Laser: http://www.intralasefacts.com.
[162] All-femtosecond laser refractive surgery - small incision lenticule extraction (SMILE): http://www.zeiss.com/meditec/en_de/products-solutions/ophthalmology-optometry/cornea-refractive/laser-treatment/femtosecond-laser-solutions/relex.html.
[163] Sano T, Mori H, Sakata O, Ohmura E, Miyamoto I, Hirose A, Kobayashi KF. Femtosecond laser driven shock synthesis of the high-pressure phase of iron. Appl. Surf. Sci. 2005, 247, 571–576.
[164] Vailionis A, Gamaly EG, Mizeikis V, Yang W, Rode AV, Juodkazis S. Evidence of superdense aluminium synthesized by ultrafast microexplosion. Nat. Comm. 2011, 2, 445.